**A review of sand detachment in modern deep marine environments: analogues for upslope stratigraphic traps**

*Running head: Detached seafloor sands*

John W. COUNTS (*jcounts@usgs.gov*)[a,b,c]

https://orcid.org/0000-0001-7374-6928 (Corresponding author)

Lawrence AMY (*lawrence.amy@ucd.ie*)[b,c]

https://orcid.org/0000-0001-7502-6887

Aggeliki GEORGIOPOULOU (*a.georgiopoulou@brighton.ac.uk*)[c,d]

https://orcid.org/0000-0003-4298-5090

Peter HAUGHTON (*peter.haughton@ucd.ie*)[b,c]

https://orcid.org/0000-0002-0567-777X

[a]*U.S. Geological Survey, Geology, Energy, and Minerals Science Center, 12201 Sunrise Valley Dr., Reston, VA, 20191, USA (current address)*

[b]*School of Earth Sciences, University College Dublin, Belfield, Dublin 4, Ireland*

[c]*Irish Centre for Research in Applied Geosciences (iCRAG), O'Brien Centre for Science, University College Dublin, Belfield, Dublin 4, Ireland*

[d]*School of Environment and Technology, University of Brighton, Lewes Road, Cockcroft Building, BN2 4GJ, Brighton, United Kingdom*

**Keywords:** deepwater; sand; sedimentation; seafloor; deposition; petroleum; seismic; analog

**Abstract**

Isolated, detached sands provide opportunities for large-volume stratigraphic traps in many deepwater petroleum systems. Here we provide a review of the different types of sandbody detachments based on published data from the modern-day seafloor and recent (generally Quaternary-present), shallow-buried strata. Detachment mechanisms can be classified based on their timing of formation relative to deposition of the detached sandbody as well as their process of formation. Syndepositional detachment mechanisms include flow transformation associated with slope failure (Class 1), turbidity current erosion (Class 2), and contourite deposition (Class 3). Post-depositional detachment is related to subsequent erosive processes and truncation of the pre-existing sandbody, either by submarine channels (Class 4), mass-transport events (Class 5), post-depositional sliding or faulting (Class 6) or bottom currents (Class 7). Examples of each of these mechanisms are identified on the modern seafloor, and show that detached sandbodies can form at different locations along the continental slope and rise (from upper slope to basin floor), and between or within different architectural elements (i.e., canyon, channels and lobes). This variation in formation style results in detached sands of highly variable sizes (tens to hundreds of kilometres) and geometries across and along the depositional profile, which are dependent upon the erosive and/or depositional processes involved, as well as the seafloor topography of the area in question. Whilst modern seafloor systems may not always represent the final stratigraphic architecture in the subsurface, they provide important insights into the development of detached sandbodies and therefore serve as potential analogues for subsurface stratigraphic traps.

## 1. Introduction

In deepwater environments, sandbodies may become physically detached from more extensive, proximal sandy deposits, leading to updip pinchouts that have the potential to form stratigraphic traps for fluids in the subsurface. These traps are an important target for hydrocarbon exploration in many basins globally (Pettingill, 1998; Prather, 2003; Fugelli & Olsen, 2005; Biteau et al., 2014; Stirling et al., 2018; Dolson et al., 2018; Zanella and Collard, 2018; Amy, 2019). This play type offers the potential for giant world-class oil fields, making them a major focus in deepwater drilling environments where high-rate, high-ultimate-recovery reservoirs are required to satisfy economic thresholds for commercial success (Weimer & Pettingill, 2007). Over the last decade Cretaceous and Tertiary deepwater turbidite complexes have been extensively drilled in passive margin settings, especially on both sides of the equatorial Atlantic (Flinch et al., 2009; Dailly et al., 2013; Kelly & Doust, 2016). Prominent recent discoveries with stratigraphic traps (pure or combined), include the offshore Ghana Jubilee Field (~600 MMBO) (Dailly et al., 2017), offshore Guyana Liza Field (800-1400 MMBO) (Alleyne et al., 2018) and offshore Senegal Fan-1 discovery (P50 of 950 MMBO) (Dolson et al., 2018).

Widespread success in this play type, however, has been difficult to replicate. For instance, Zanella and Collard (2018) note that out of sixty-eight post-Jubilee exploration wells drilled on the African Transform Margin, only two resulted in development projects. The presence of a robust trap to prevent updip leakage of hydrocarbons is often considered one of the highest risks associated with pinchout plays (Straccia & Prather, 1999; Prather, 2003; Fugelli & Olsen, 2005; Loizou, 2014). The risks associated with updip pinchout of reservoirs on the proximal parts of the depositional profile (upslope stratigraphic traps *sensu* Amy, 2019) is likely to be especially high, given the potential for relatively coarse-grained and continuous slope deposits in slope channel complexes or canyons. A failure analysis of recently (2008-2017) drilled stratigraphic prospects worldwide concluded that one of the major causes of geological failure is the lack of effective closures and seals (Zanella and Collard, 2018). Similarly, a 2015 assessment of exploration well failures in the UK North Sea found that a lack of seal or trap closure was a significant cause of failure (>50%) in Jurassic deepwater turbidite prospects (Mathieu, 2018). These results suggest that, despite significant advances in seismic imaging, the ability to predict deepwater stratigraphic prospects with robust closure and containment elements remains limited.

In this study, we provide a review of processes that can cause sand detachment on the seafloor, as suggested by data from modern and shallowly buried seafloor systems. Seafloor data is able to provide information on planform geometries over large areas (tens to hundreds of $km^2$), usually difficult to achieve in outcrops, with higher resolutions compared to industry seismic datasets. Furthermore, seafloor systems may be more easily understood with regards to their depositional and geologic setting, helping to constrain the location of detachment along the slope profile and the probable controls on formation. In this review, we primarily focus on relatively large-scale, coarse-grained (sand and gravel) sandbodies with updip terminations, either pinchouts or erosional truncations, that could offer analogues for large-scale upslope stratigraphic traps and giant oil/gas field potential in the subsurface. Examples presented here are generally Quaternary to present age, with the inclusion of selected older examples where necessary. The objectives of this work are to: i) provide an overview of the methodology and terminology used to identify detached sandbodies in modern seafloor systems; ii) present a process-based classification scheme for different types of pinchout type exemplified by selected cases; and iii) discuss the processes and location of detachments along the depositional profile, the effectiveness and preservation potential of different detachment mechanisms, the controls on detachment, and the implications for exploration.

## 2. Methodology and Terminology

Literature on seafloor systems was reviewed in order to collate examples of detachment at the proximal updip edges of sandbodies in recent deepwater systems. Examples of detachment discussed herein are drawn from over 20 localities across the globe (**Fig. 1**). These span a wide range of geologic settings, including passive and active continental margins, active and inactive depositional systems of varying dominant grain sizes, and differing proximity to fluvial sources. In this review, we have considered detachment along the depositional profile from the continental shelf-slope break to the abyssal plain, but have excluded shallow marine shelf environments. Here we focus on "recent" systems, including both deposits that are visible on the modern seafloor surface, as well as those that are shallowly buried; and outcropping systems are generally not considered in this review. Deeply buried (i.e., hundreds of meters or greater) examples of subsurface stratigraphic traps have received detailed treatment elsewhere, including by Amy (2019), who comprehensively reviewed and classified numerous examples. Direct comparison of the detachment mechanisms described herein with ancient outcropping deposits is often problematic due to the lack of oceanographic and geographic context and uncertainties in the specific sedimentological processes involved at the time of deposition for the latter. Additionally, ancient sandbodies often cannot be accurately assessed as being 'detached' due to the two-dimensional nature of their exposure. Inclusion of such examples would therefore necessitate a discussion of these uncertainties that is beyond the scope of this study.

The concepts of attachment and detachment are applied in this paper in a broader sense than generally considered in previous work which has primarily focused on the morphological or stratigraphic continuity between slope channels and basin-floor fans or lobes due to sediment erosion and bypass by turbidity currents (e.g., Mutti & Normark, 1987; Mutti, 1992; van der Mewe et al., 2014; Hansen et al., 2019; Wynn et al., 2002a). "Detachment" is defined here as the lack of physical continuity of slope or basin floor sands with more proximal sand-dominated (or other permeable) units, including shelf and fluvial deposits, caused by sediment erosion or by sediment "bypass" (non-deposition) by turbidity currents or other sediment transporting flows. Sediment erosion may occur contemporaneously with deposition of the detached sandbody, or by later events that sever the physical continuity between the up-dip and down dip sandbodies. For detachment to occur, depositional units or elements (e.g., channel, lobes, sheets, drifts, etc.) must "pinchout" (i.e. gradually thin to zero or be abruptly truncated). A “detached depositional system” (*cf*. “Type I of Mutti, 1985; see Van der Mewe et al., 2014, for a review of terminology) is a turbidite system with one or multiple upslope-detachment points and in the subsurface would offer stratigraphic closure for hydrocarbon accumulation but not necessarily containment (i.e. robust base, lateral or top seal). In contrast, an “attached depositional system” lacks any upslope detachment points from its distal margin to the fluvial or shelf feeder system and thus offers no updip stratigraphic closure moving proximally upslope.

The examples described herein either contain sufficient data that allow detachment of sands to have been interpreted by the original author(s) of the cited work, or, where noted, inferred from our own analysis. Recognised seafloor examples of detached sandbodies are located downslope of zones of erosion or non-deposition (i.e., where the seafloor is composed of exhumed older sediments or bedrock) or mud-prone facies (e.g., mass transport deposits). Seven main categories of detachment were recognized. Detachment examples were classified, and are described below, according to i) their timing of detachment relative to deposition, and ii) the processes responsible for detachment (**Fig. 2**). “Syndepositional” detachment refers to scenarios in which the sandbody in question is *initially* deposited in a state of detachment (i.e., separated from the proximal shelf by a zone of non-deposition, erosion, or by deposits of fine-grained sediment). “Post-depositional” detachment is the result of erosional truncation of an existing attached deposit. Each mechanism is described further below with examples from the modern seafloor and shallowly buried recent deepwater systems.

## 3. Results

### 3.1 Syndepositional detachment processes and examples

#### *3.1.1: Class 1: Debris flow transformation*

Turbidity currents in the marine environment may be triggered by a number of processes, including catastrophic slope failure (Mohrig and Marr, 2003). In such events, turbulent mixing of mass flows or debris flows with ambient fluid is responsible for turbidity current generation (Felix and Peakall, 2006) and hydrodynamic segregation of sand, sometimes forming clean sands in more distal locations (e.g., Kastens, 1984). Many of the largest mass-transport deposits on the seafloor (those with high volumes and wide spatial distributions) initially begin as slope failures, and often transition later into debris flows and then turbidity currents, (Fisher, 1983; see also for example Talling, 2014). Clean, sandy turbidites generated through this process can be detached by intervening updip mud-prone mass transport deposits (e.g., slumps and debrites) and, confined or sealed laterally by fine-grained deposition the open slope (**Fig. 3A**) or within a canyon or channel (**Fig. 3B**). These result in different scales and morphologies of the failure zone, transfer zone, and resulting sandbody. Open slope failures may have a lower likelihood of reattachment compared to in-canyon/channel failures, though the axes of canyons sometimes contain sand or gravel lags that may promote connectivity, especially in smaller events where the canyon is not flushed completely.

Examples of large, detached, failure-generated turbidite deposits with intervening debrites are well-documented in the modern submarine environment. For example, the Holocene reactivation of the Sahara Slide headwall on the NW African margin (**Fig. 3C, 3D**) resulted in sandy turbidites at distances of over 700 km from the original source, separated from the shelf by approximately coeval debrites and mud-rich hybrid event beds. In this case, the slope failure complex is comprised of multiple headwall scarps, downdip of which are blocky, thin translational slide deposits as well as thick, poorly sorted debrites chaotically mixed with clasts of hemipelagic oozes and rare sands (Frenz et al., 2008; Georgiopoulou et al., 2009), each with kilometre-length scales. These intervening deposits separate the proximal shelf from sandy turbidites on the basin floor that consist, in part, of massive or slightly fining-upward, well sorted sands (Bouma *Ta* and *Tb* divisions shown in core profiles in **Fig. 3C**). A separate, but adjacent debris flow event (the Canary Debris Flow, illustrated with a dashed outline in Fig. 3C), also resulted in turbidite formation and the segregation of sands into distinct beds. In this example, deposits referred to as the “B” turbidite are present on the Madeira Abyssal Plain (labelled in **Fig. 3C**) distal to the outlined debrite (Masson et al., 1997; Weaver et al., 1995). Other potential examples include the Storegga Slide complex (offshore Norway), one of the largest submarine landslides known, which contains both updip debris flows (Haflidason et al., 2004) and turbidites with internal sand-dominated units (Bugge et al., 1987).

*3.1.2: Class 2: Turbidity current erosion and bypass*

The erosive power of turbidity currents is well established (Weaver and Thompson, 1993; Mayall et al., 2006), and turbidity currents that bypass or erode proximal parts of their flow path have been identified in several ancient systems (e.g., Mutti, 1977; Brooks et al., 2018). This process can result in detached sandy turbidite deposits downdip of the bypass zone, each of which may have unique characteristics depending on the exact setting.

3.1.2.1: Class 2A: Erosion and bypass in channels or canyons

In deepwater fan systems, sands may be detached when turbidity currents fully erode or completely bypass parts of the slope system, in contrast with Class 1 where detachment occurs due to updip facies changes. In this scenario, detachment may be considered the result of 'high efficiency' flows (*sensu* Mutti and Normark, 1987) that are able to locally transport most of their sediment load basinward without significant deposition (**Fig. 4A**). Bypass and discontinuous deposition can happen within a channel itself when gradient changes in an uneven or stepwise fashion, as in the case of the Stromboli slope valley system (Gamberi and Marani, 2007), or in the form of lobate bodies and/or spillover fans in low-gradient areas (**Fig. 4B**). Repeated erosional flows over time may result in erosional or mixed (rather than depositional) submarine channels (Clark and Pickering, 1996), expressed on the seafloor by a V-shaped cross-sectional morphology and lack of infill (Covault, 2011). However, channels preserved in the geologic record often show that erosional cutting phases are sometimes followed by sediment backfilling, a process that has complex allocyclic and autocyclic controls, including base-level changes (MacPherson, 1978; Bruhn and Walker, 1995; Cronin et al., 2005). Thus, while sands may be deposited in a detached state in the course of a single turbidity flow event, full detachment of a turbidite lobe, lobe complex, or in-channel sand body requires that the process occur consistently and be preserved over time.

Examples of systems with discrete abandoned channels and lobes are found in the modern Congo/Zaire (Babonneau et al., 2002; Manson, 2009, Picot et al., 2016), Mississippi (Stelting et al., 1986), Bengal (Schwenk and Speiss, 2009; Emmel and Curray, 1983), and Amazon (Pirmez and Flood, 1995; Jegou et al., 2008); at least some of these abandoned elements may be detached from their proximal sources. Additionally, lobes in the Monterey fan system, offshore California, have been interpreted as being detached (Fildani and Normark, 2004), offering a modern example of the process. Bypass and erosion can also be demonstrated through bed-scale correlation of a deposit resulting from a singular event, as has been documented in the Agadir Basin, offshore of Morocco, by Stevenson et al. (2015). Here, bypass is demonstrated by the absence of "Bed 5" (ca. 60 ka) within the axis of the northern Madeira Channel System, where its deposits (including fine-grained sands) are present both in more proximal and distal locations, separated by multiple bypass zones (**Fig. 4B**). These bypass zones may have lengths of >10's to >100 km, implying sustained bypass or erosion over a large area. The more proximal bypass zone occurs in association with a channel-lobe transition zone (CLTZ), discussed further below. Another example comes from the 2016 submarine sediment gravity flow that was triggered by a magnitude 7.8 earthquake near Kaikōura, New Zealand. This flow flushed Kaikōura canyon of 360-850 Mt of pre-existing sediment and eroded up to 40 m of the canyon floor before depositing a detached sandy turbidite downslope in the Hikurangi channel (Mountjoy et al., 2018).

3.1.2.2: Class 2B: Erosion on stepped and complex slope profiles

Erosion and bypass may also occur locally on topographically complex slopes, where sands fill bathymetric lows on the seafloor but are not deposited in intervening high-gradient areas (Smith, 2004; Brooks et al., 2018; **Fig. 4C**). In this scenario, the detachment process is the same as that described in 2A above, though the differing slope morphology leads to a different geometry of both the detached deposit and the bypass zone. The most well-known examples of this are in the Gulf of Mexico, where salt withdrawal at depth creates seafloor depressions (minibasins) in which turbidite sands are ponded, forming thick, sandy reservoir deposits. Once accommodation is reduced or no longer available, sands bypass and are transported into another downslope minibasin through incised channels (**Fig. 4D**; Winker, 1996). Bypass and erosion are common in these channels, allowing individual minibasin deposits to be detached from one another and from surrounding slope sediments (Prather, 2003). Similarly, complex slope topography and stepped, detached minibasins can also result from active margin tectonic processes. Imbricate thrust zones within accretionary terranes can result in multiple slope-parallel thrust ridges, separated by trench-slope minibasins in which sedimentation is concentrated; uplift of thrust ridges provides a physical barrier to deposition, facilitating detachment. This scenario is exemplified on the Hikurangi margin (offshore New Zealand), where the subducting Pacific plate creates an accretionary wedge and a minibasin-thrust ridge system on the eastern side of the island (Lewis, 1980). Minibasin fill is dominated by fines, but periodically punctuated by thin, earthquake-triggered turbidites with basal sands, which are not always present on ridge highs (Lewis and Kohn, 1973).

3.1.2.3: Class 2C: Erosion within channel-lobe-transition zones

The CLTZ has often been considered an optimal location for enhanced erosion and sediment bypass and hence a possible detachment point. At this location, changes in flow properties resulting from reduced gradient and/or lack of channel confinement may force flows to thicken and slow, causing a hydraulic jump as they move onto the basin floor (**Fig. 4E**; Komar, 1971; Mutti and Normark, 1987; Wynn et al., 2002a; Pohl et al., 2019). The enhanced turbulence associated with a hydraulic jump is inferred to be an important process responsible for seafloor features with distinct morphologies (e.g., scours and bedforms) that characterise some CLTZs (Normark and Piper, 1991; Wynn et al., 2002a).

Examples of CLTZs and associated features have been documented from several localities on the modern seafloor, including from early studies using side-scan sonar imagery (Normark, 1978). However, despite recent advances in the acquisition of seafloor sedimentological data, complete, detailed studies of CLTZs in modern environments (with a full understanding of the processes and deposits involved) are still uncommon. Wynn et al. (2002a) presented three case studies of CLTZs in the Atlantic and Mediterranean: the Agadir, Lisbon, and Rhone systems. Scour morphology and scale differs across each of these systems, and the size of the CLTZ is proportional to the size of the system, though all are on the order of 10's of kilometres. Each zone contains erosive features, including isolated and amalgamated scours, lineations, and scarps. Individual scours in these systems are <1-3 km long and 10's m deep (Rhone neofan scours shown in **Fig. 4F**, from Bonnel et al., 2005), and may coalesce into amalgamated scours up to 9 x 6 km, although these may contain topographically elevated remnants of past deposits that were not fully eroded. In the central and distal parts of CLTZs, patchily distributed depositional features including sediment waves, mounds, and sand streaks, may also occur such that the CLTZ is not purely an erosional zone. MacDonald et al.'s (2011) catalogue of large-scale erosional scours associated with CLTZs shows that individual scours can be long-lived (up to 200 kyr) features and can be partially filled with sediments that may comprise a combination of mass transport deposits, sandy turbidites and intervening pelagic muds. In the Valencia Fan (eastern Mediterranean), discontinuous scours are present in conjunction with isolated sand ribbons and dunes (Palanques et al., 1995). These examples generally show a proximal-distal transition from large to smaller scours, to coarse-grained sediment mounds, to thin, streaky reworked sands, and finally to more continuous lobe deposits. In the most recent deepwater lobe of the Nile deep sea fan, the zone between the most distal portion of the channel and the generally fine-grained lobe is characterized by a smaller sandy lobate body (visible in backscatter in **Fig. 4G**; Migeon et al., 2010) without clear evidence of scouring or erosion. Erosion in CLTZs may therefore be incomplete, and the spatial distribution of sediments likely to change with successive flow events on account of variable flow characteristics, increasing connectivity risks.

3.1.2.4: Class 2D: Erosion or bypass associated with crevasse splay formation

Breaching of levees in submarine channels can result in the deposition of basin-floor sands in the form of crevasse splays (**Fig. 4H**) or in the case of spillover due to flow stripping where sand is suspended above the levee crest (Piper and Normark, 1983). Detachment may occur due to erosion/bypass between the channel and the splay deposit, or by incomplete breaching of levees, where finer-grained levee deposits may remain between the channel and splay deposits. Crevasse splays have been observed on both the modern seafloor (Twichell et al., 1996), and in the shallow subsurface of the Gulf of Mexico (Posamentier et al., 2007), the northeastern Pacific (**Fig. 4I**; Gardner, 2017) and the Bay of Bengal (Lowe et al., 2019) among other localities. In the Bay of Bengal, amplitude extraction from 3D seismic data reveals a possible zone of bypass in the area closest to the feeder channel, suggesting that splay sands may be detached (Lowe et al., 2019). Avulsion and crevassing may be followed by further channel development atop the initial splay deposit, with the latter preserved as a laterally extensive coarse-grained unit that forms a repeated component of channel architecture (high-amplitude reflection packet, or HARP) in, for example, the Amazon fan system (Flood et al., 1991; Damuth, 2002).

*3.1.3: Class 3: Bottom current deposition and winnowing*

Once in the marine environment, sand-sized particles may be remobilized and redeposited by deepwater bottom currents, forming bottom-current reworked sands (BCRS) (de Castro et al., 2020), which may be isolated in the deep sea and detached from their original sediment input source. Sands are often sourced from nearby turbidite systems, and bottom currents often interact with downslope turbidity currents at transverse angles to form mixed or hybrid systems within a basin (**Fig. 5A;** Rebesco et al., 2014, Faugères and Mulder, 2011). Detached sands may form at multiple locations within these types of systems, including the upper and middle slope as slope-parallel currents strip sediment from downslope flows and transport it laterally along contourite-generated terraces. Similar processes occur in more distal locations (i.e., on the lower slope) due to reworking of turbidite lobes (de Castro et al., 2020). Winnowing of fines by bottom currents throughout turbidite systems potentially improves reservoir quality of both attached and detached sands (e.g., Fonnesu et al., 2020).

Detached sandy contourites have been well-documented in the Gulf of Cadiz (Nelson et al., 1993; Hernández-Molina et al., 2003; Llave et al., 2007; Brackenridge et al., 2018; de Castro et al., 2020), where mixed-source sediment is moved and redeposited by currents of Mediterranean Outflow Water exiting the Strait of Gibraltar. Here, contourite features are distributed around the mid-slope into a number of different provinces, each of which is characterized by dominant morphologies and sediment types. Contourite depositional systems with a sand component may be present in the form of mounded, sheeted, or elongate drifts, with scouring and erosional features also common throughout the region (Hernández-Molina et al., 2003). Meter-scale thick, continuous sands are seen in northern and southern arms of the Cadiz Contourite Channel, with a general decrease in sand content away from channel axes (Brackenridge et al., 2018). Other examples of sandy contourites are found in the Gulf of Mexico (Shanmugam et al., 1993), the Argentine continental margin (Bozzano et al., 2011), and in the subsurface (Pleistocene; location unrecorded); (Viana, 2008). The subsurface example illustrates the preservation potential of the mechanism, with a complex of avulsion lobes that have been reworked into smaller, irregular sandbodies (**Fig. 5B**). These examples each have deposits related to both bottom current and turbidity flow processes, forming mixed systems.

### 3.2: Post-depositional detachment processes and examples

A number of mechanisms involving erosion and/or reworking may detach sands after their initial seafloor deposition. These processes generally involve only limited depths of erosion to several tens of meters, and typically occur at time scales of 0 (near-instantaneous) up to $10^6$ years.

#### *3.2.1: Class 4: Erosion by slope turbidite channels*

On the lower slope, many canyons transition into sinuous deepwater channels, which can continue basinward for hundreds or even thousands of kilometres (Covault et al., 2012) and may incise tens of meters into the seafloor (e.g., Babonneau et al., 2010; Deptuck and Sylvester, 2018). The crosscutting of one submarine channel by another provides a potential mechanism for the detachment of downdip basin-floor sands. In this scenario, complete detachment requires: 1) the abandonment of the initial, earlier sand-dominated channel, 2) crosscutting and erosion by a subsequent channel, to a level deeper than the initial channel, and 3) the filling of the later crosscutting channel with muddy deposits conducive to seal formation (**Fig. 6A**). In such scenarios, however, many opportunities exist that may allow detachment to be compromised. Most notably, submarine channels often contain coarse-grained lags or bars emplaced along their length (Janocko et al., 2013), even those considered to be in a bypass or erosional regime. Additionally, sands may be deposited outside of channel axes through flow stripping and crevassing. If such deposits were continuously present in or around the later crosscutting channel, they may result in a persistent attachment.

On the modern seafloor and in the shallow subsurface, mapped submarine channels within fan systems show numerous instances where younger channels intersect previously abandoned channel segments (e.g., those in **Fig. 6B**; Jegou et al., 2008). However, neither the degree of incision nor the nature of channel fill is always clear in these types of data sets. Evidence for mud-filled channels that crosscut sand-filled channels is best observed in older subsurface systems, where infilling sediment character along a continuous area can be inferred from seismic reflection amplitudes (e.g., **Fig. 6C**).

*3.2.2: Class 5: Erosion by mass transport events*

Slope failures and subsequent mass transport processes can result in decameters of erosion on the seafloor of many 10s of metres depth (Eggenhuisen et al., 2010; Dakin et al., 2013; Sobiesiak et al., 2018), and can therefore isolate and detach previously deposited sands from the shelf and slope. Mass transport deposits (MTDs), for example, have been observed to locally erode the proximal portions of slope channels and lobe complexes, resulting in distal sands that are decapitated from their source through slope erosion and the emplacement of large-scale MTD (**Fig. 7A**).

Channels terminating updip into MTD and slope failure scars can be clearly seen in the western Nile delta near the Rosetta lobe (**Fig. 7B**). Here, multiple slope failures during the Pleistocene-Holocene triggered a series of mass transport events originating from east of the Rosetta canyon (Garziglia et al. 2008). While the most recent, active channel is not affected by the slide, at least two well defined paleochannels (channel-levee systems 3 and 5 of Garziglia et al., 2008) have portions of their channel axes completely removed by mass transport events. These channels are inferred to be sand-filled downdip of MTD erosion and to terminate distally in sandy lobes (Ducassou et al., 2009). Moscardelli et al. (2006) also document erosional scours up to 30 m deep that were formed by large mass transport events in offshore Venezuela, helping quantify the magnitude of erosion resulting from these processes.

Erosive mass transport events can also occur within submarine canyons rather than on open slopes. These are more likely to interact with existing fan systems, although given their smaller volume, they are unlikely to completely destroy the upper parts of sandy turbidite complexes. In-canyon wall failures are present in most submarine canyons (e.g., Iacono et al., 2011; Chaytor et al., 2009; Janocko et al., 2013; He et al., 2014, Gardner et al., 2016, and many others), though due to their smaller scale, they are more likely to simply impede connectivity by partially eroding and blocking parts of sandy deposits rather than detaching downdip sands.

*3.2.3: Class 6: Translational failure of upper slope sandy systems*

Sandbodies deposited onto continental slopes in canyon floors, channels and associated deposits, or as lobate bodies may become disconnected from the proximal shelf if the slope fails (**Fig. 8A**). In this case, we assume that relatively limited internal deformation or disaggregation occurs, and that turbidite sandbodies maintain their original characteristics and reservoir viability. Unlike Class 5, in which the sand body is truncated by an erosive MTD, here, failure may occur along a subsurface glide or shear plane, or early syndepositional fault, and the entire sand body may be translated basinward while still maintaining coherency. Detached sands may be contained within slides, slumps, or as coherent blocks within MTDs. Examples of basinward transport processes with some translational component can be found both in the subsurface and in more recent settings. International Ocean Discovery Program (IODP) core acquired within the Tuaheni Landslide Complex (offshore New Zealand) reveals the presence of undeformed or lightly deformed bedding, including meter-scale beds of sands, within a large MTD that originated on the Hikurangi margin (Pecher et al., 2018; Couvin et al., 2020). Bedding (including sands) is interpreted to remain relatively organized due to its inclusion in undisturbed or incipiently slumped blocks of stratified sediment that are transported downslope by the MTD (**Fig. 8B**), which terminates into a headward scarp (Couvin et al., 2020). In the Porcupine Basin offshore of western Ireland, subsurface data has revealed downslope slumping of Lower Cretaceous sediments, creating an upper slope detachment zone that can clearly be seen to separate slope deposits from those more proximal (Pedley et al., 2015; **Fig. 8C**). RMS amplitude extraction maps for individual horizons show detached lobate bodies interpreted as turbidites; amplitude brightening associated with updip closure may suggest the presence of potential reservoirs created by this type of stratigraphic trap.

*3.2.4: Class 7: Erosion by bottom currents*

Bottom currents may also be responsible for erosion, which may be considered distinct from the reworking and reposition described in Class 3. Bottom currents may also erode and winnow fine-grained sediments, leaving behind sands and coarse-grained particles (Stow et al. 2008). In the Gulf of Cadiz, bottom currents are observed to be responsible for deep, erosive, slope-parallel channels and/or moats (100's of meters deep on the present-day seafloor) at the base of slope where currents associated with the Mediterranean Upper Water are forced against the slope by the Coriolis effect (**Fig. 5A, Fig. 9**; see Rebesco et al., 2014, and Hernández-Molina et al., 2008 for a review). These linear channels and moats may separate deposits of the lower slope from those on the upper slope and shelf, including many sandy mixed contourite/turbidite deposits (Hernández-Molina et al., 2016); their slope-parallel orientation increases the likelihood that they will intersect sand-dominated downslope delivery systems. Slope contourites in the Argentine Basin are also separated from the shelf and upper slope by linear erosive zones; instead of terminating in a basal lobe, slope canyons abruptly disappear into a series of slope-parallel contouritic channels caused by the northward flow of Antarctic Bottom Water (Hernández-Molina et al., 2009), illustrating their capability to erode sand. Like Class 4, long-term detachment due to bottom current erosion is dependent upon the filling of channels, moats or other eroded zones with fine-grained sediment; this would require some degree of reorganization of bottom currents and a cessation of sand input from the slope.

## 4: Discussion

Previous work on sand detachment in deep-marine environments has principally considered connections between seafloor channels and lobes, as dictated by erosion and bypass processes in turbidity currents (Mutti & Normark, 1987; Mutti, 1992; Wynn et al., 2002a; Van der Merwe et al., 2014; Stevenson et al., 2015). Here, we have reviewed existing literature on modern seafloor systems in order to broaden and classify the range of marine sedimentary processes that can result in updip terminations of sandbodies based on the process and timing of detachment (**Fig. 2**). The occurrence of one or more of these processes are a prerequisite for the formation of large-scale stratigraphic traps in the subsurface, however, each process may differ in its effectiveness, location and preservation potential; all are factors to consider when evaluating trapping risk.

### *4.1: Detachment Effectiveness*

Formation of a robust pinchout or truncation is key to effective detachment. Based on observations reported here, some mechanisms are considered to be more likely to result in complete detachment than others. These more effective mechanisms include flow-transformation-related sands (Class 1), especially where downdip clean sands are separated from shelf sediments by slope collapse zones (MTDs) and failure scars. Detachments related to MTD erosion (Class 5), where mud-prone mass flows with seal capacity create deep erosion (e.g. Cardona et al., 2016), should also form robust detachments. Conversely, while the CLTZ has been discussed as an optimal site of potential detachment (Mutti & Normark, 1987; Mutti, 1992; Wynn et al., 2002a; Van der Merwe et al., 2014; Stevenson et al., 2015), seafloor data indicates that CLTZ zones are not always present between channel and lobes. When present, CLTZ's may contain sand and gravel deposits, often in between or within erosional scours and small channels (Wynn et al., 2002b; Stevenson et al., 2015; Postma et al., 2016). Moreover, some CLTZ examples, such as those seen in the Rosetta lobe of the Nile system (Migeon et al., 2010) are not wide enough to separate channel from lobe deposits. Given the dynamic nature of this zone, CLTZs may be preserved as continuous or semi-continuous lag deposits, which have been identified in outcrop (Van der Merwe et al., 2014; Postma et al., 2015; Hofstra et al., 2018). Outcrop data suggest relatively high net sand values for interpreted CLTZ deposits and greater lateral continuity than channel and lobe deposits (Fryer & Jobe, 2019). Thus, we suggest that CLTZ-related stratigraphic traps be considered high risk; a supposition also supported by the lack of examples of stratigraphically trapped producing reservoirs associated with CLTZ pinchouts (Amy, 2019).

Another critical factor for stratigraphic trapping potential is the overall amount of net sand in the slope system. Whilst higher net-to-gross, active margin systems afford better reservoir potential, it may significantly compromise the chance of stratigraphic trapping (Reading and Richards, 1994). Analysis of seafloor systems shows that relatively coarse-grained systems, despite having high gradient slopes, likely have limited updip pinchout potential. For instance, sands and gravels appear to form a continuous body of sand and/or gravel within the axes of slope canyons and channels in the cases of the Var (Klaucke et al., 2000) and Monterey (Paull et al., 2005) systems. However, detachment of small scale sandbodies might occur locally in these systems, as associated with cyclic steps on the Var ridge (Migeon et al., 2000; Cartigny et al. 2011). Passive margins often favour the development of large, muddy fan systems (Reading and Richards, 1994; Bouma, 2004). Such muddier systems should be more prone to bypass, since it is easier for currents to suspend and bypass finer-grained particle sizes promoting erosional regimes on slopes (Mutti and Normark, 1987; Amy & Dorrell, in review), however, they will also be prone to lower reservoir potential due to the overall increased amount of fines in the system.

In both detachment scenarios related to bottom-currents, the specific sediment inputs, current directions and velocities, and basin topography preclude an overall assessment of detachment effectiveness. Bottom-current erosion, however, may be generally more effective and predictable than deposition (assuming the presence of existing sands) as it is known to occur in slope-parallel moats and channels that may have significant relief and temporal persistence (Stow et al. 2008).

### *4.2: Detachment Location*

The amount and coverage of geophysical data currently does not allow a quantitative analysis of whether detachment is more likely to occur in certain locations along the slope, or along certain margin types. However, while the nature and location of each individual detachment zone is specific to the sedimentary, physiographic, and oceanographic system in which it occurs, some generalizations can be made about the most likely location of erosive, bypass, or transfer zones based on knowledge of the processes involved. **Figure 10A** schematically illustrates and summarizes the various detachment mechanisms discussed here, and their relative locations on the continental margin. The review presented here shows that detached sandbodies (depicted in yellow) can occur widely across the slope, both in profile and laterally on different margin types. Ultimately, detachment, or lack thereof, is controlled by several factors, including: 1) the grain size and sorting of input sediment, 2) the height, frequency, and variability of the flows involved, 3) the status of the system relative to its equilibrium profile, i.e., whether the geometry of the system favours erosion or deposition, 4) the erosive capability of submarine landslides, and 5) the intensity and direction of bottom currents. These are in turn controlled by the larger-scale geologic and oceanographic setting of the area in question (e.g., active vs. passive margins; **Fig. 10A**), which affect the overall margin geomorphology, the slope gradient, the frequency of earthquakes and volcanic eruptions, and the shelf width. Pinchout location is controlled by detachment mechanism and thus, *a priori*, upper slopes of active margins with high gradients might be expected to be probable sites for slope failure and turbidity current erosion-bypass related detachments. Previous studies using seismic analysis have also made this inference (e.g., Hadler-Jacobsen et al., 2005). However, given the complex nature of these phenomena, there may not be a simple correlation between gradient and slope failure location (e.g., McAdoo et al., 2000, Krastel et al., 2012; Urlaub et al., 2015). Similarly, though turbidity current erosion and bypass is dictated by the equilibrium profile (Kneller, 2003; Georgiopoulou and Cartwright, 2013; Amy & Dorrell, in review; Crisóstomo-Figueroa et al., in press), modern systems suggest that detached sandbodies related to turbidite erosion (Class 2A, for example) form near both higher-gradient active margins as well as on low-gradient passive margins (e.g., Congo fan system; Babonneau et al., 2010) (Fig. 10A). Topographic relief leading to ponding and erosion can also be generated locally by different underlying causes (e.g., salt-related subsidence, or deep tectonic processes expressed on the seafloor). Similarly, syndepositional sliding and faulting (detachment by translational failure) is likely present on continental slopes of both active and passive margins, depending on the gradient and rheology of the slope sediment itself. The final result—detachment in Classes 2A, 2B, and 6—is therefore present across a variety of geologic settings.

Aside from those processes related to turbidity currents, the controlling factors behind other mechanisms may also lead to them to occur more frequently in certain settings. Channel crosscutting is most often found in the middle and distal portions of deepwater fans, where channels are highly meandering and prone to avulsion. Sand bed deposition resulting from flow transformation necessitates that the sediments incorporated into the initial failure contain a substantial portion of sand-sized sediment, most likely on active margins or in the vicinity of large fluvial inputs. Conversely, long-term detachment necessitates that failure scars be healed by fine-grained sediments, a point that emphasizes the complex nature of detachment and the disconnect between the modern environment and the geologic record. Finally, bottom-current related detachment should be most prominent on the margins of large open basins and portions of the slope profile impinged upon by strong bottom currents, including in and around large contouritic terraces (de Castro et al., 2020, Hernández-Molina et al., 2018).

*4.3: Preservation Potential*

Although each of the mechanisms described here carries some inherent risk when considering their probability of forming reservoirs or traps, ancient examples (known from subsurface or outcrop) of each mechanism are present in the geologic record (**Fig. 10B**). As outlined for post-depositional detachment classes, initially attached systems may evolve to become detached due to subsequent erosion. The opposite may also occur, where detached systems become attached prior to burial, posing a key risk for stratigraphic trap formation. This evolution may occur, for instance, in cases where detachment is associated with erosion/bypass by turbidity currents in channel reaches or in the proximal lobe (Class 2A). Changes in flow parameters through time may reduce the ability of flows to transfer their coarse load basinward, as related to their efficiency or equilibrium slope (Mutti, 1992; Kneller, 2003). This process can result in phases of backfilling of erosional conduits with coarse material, as described by evolutionary models for canyon and channel stratigraphic development (e.g., Gardner et al., 2000; Samuel et al., 2003; Dalla Valle & Gamberi, 2011; Bain & Hubbard, 2016; McArthur et al., 2018). Preservation of detached lower slope or basin floor sandbodies may thus be contingent on the inhibition of backfilling processes. Recent work shows the potential for updip migration of coarse-grained bedforms under supercritical flow conditions in channels and channel-lobe settings that may facilitate the development of updip thief lags or backfill feeder conduits (e.g., Postma et al., 2014; Vendettuoli et al., 2019). Similarly, slope failure-related detached sandbodies (Classes 1 and 6) may become reattached if slope systems continue to deliver coarse material to the area of detachment or become sites of slope incision exploited by new conduits (e.g., in the Rockall Trough; Elliot et al., 2006).

Producing fields with upslope stratigraphic traps demonstrate that the mechanisms described here may be preserved over geologic time spans. Known examples of fields indicate that viable traps can be produced by detachment Classes 2, 4, 5 and 6 of this study. These include reservoirs whose updip pinchouts are inferred to have been produced by turbidity current bypass (e.g., Alba, Buzzard, and Young North fields) and post-depositional erosion by submarine channels (e.g., Marlim, Marlim Sul, and Shwe fields) or mass transport erosion (e.g., Bud, Nautilus, Pabst fields) (Amy, 2019). Plays exploiting contourites have also been identified by Shanmugam et al. (1993). Examples of commercial hydrocarbon volumes trapped in pinchouts associated with the other detachment mechanisms (Classes 1, 3 and 7) are lacking; conspicuously absent are examples of producing fields of upslope stratigraphic traps associated with CLTZ processes. As found in modern systems, upslope pinchouts in stratigraphically trapped fields occur along the slope profile, from the upper to the lower slope (Amy, 2019). Anecdotally, the significant potential for deepwater stratigraphic traps in the subsurface is supported by the recent assessment that more oil and gas have been discovered in upslope stratigraphic traps than any other type (Myers, 2020). However, it should be noted that only a relatively small number (~20) of producing fields with upslope stratigraphic traps have been reported (Amy, 2019). The paucity of field examples may be attributed to a range of factors, including those that are not geological in nature (i.e., confidentiality and/or commercial and exploration strategy).

## 5: Conclusions

The wide array of detached sandbody types found on the modern deep seafloor and in the shallow subsurface defines the range of possible stratigraphic closures in buried deepwater systems. Detachment may occur simultaneously with the event(s) that deposit sandbodies themselves, or by subsequent erosive processes that can disconnect initially attached systems. Deepwater syndepositional detachment processes include flow transformation (Class 1), turbidity current erosion (Class 2), and deposition of sands by bottom currents (Class 3). Post-depositional detachment processes include erosional turbidite channels (Class 4), truncation by mass-transport deposits (Class 5), downslope translational movement due to slope failure (Class 6), and erosion by bottom currents (Class 7). The diversity of these processes results in detachment zones that vary in size and effectiveness, and in detached sands that may occur throughout the slope profile and across margin types. Whilst recent systems may not represent the final stratigraphic architecture, they provide important insights into the development of detached sandbodies that offer stratigraphic-trap potential in analogous subsurface systems.

## FIGURE CAPTIONS

**Figure 1**: Global map (bathymetry/topography) of selected locations mentioned in this study. Sites color coded by detachment mechanism. Class numbers are defined in more detail in Fig. 2; basemap from Amante and Eakins (2009).

**Figure 2**: Top-tier classification of detachment mechanisms discussed in this paper. Classes are based on timing of detachment relative to initial sandbody deposition; subclasses (discussed in text) are related to more specific processes and settings that may affect the morphology and sedimentological properties of the final deposit. Red boxes in Classes 3 and 7 highlight specific process in questions (erosional vs. depositional).

**Figure 3**: Illustration and examples of Class 1, detachment through flow transformation. A) Open-slope failure unrelated to existing channel-canyon system, creating large, sometimes basin-scale turbidite deposits. B) Failure of steep canyon walls or upper slopes, where sediments are directed into pre-existing canyon and channel systems. Resulting turbidite deposits overlie those in the channels and lobes that are the result of previous turbidity currents. C) Map of the Sahara Slide and Canary Debris Flow, offshore northwest Africa, showing scale of deposits interpreted to have undergone flow transformation and location of cores containing evidence of differing downslope processes. Modified from Georgiopoulou et al. (2009, 2010) and Weaver et al. (1995). D) Schematic cross-section A-A’ in Figure 3C, showing interpreted flow transformation process and slope gradient for the Sahara Slide. Modified from Georgiopoulou et al. (2010).

**Figure 4**: Detachment related to erosion by turbidity currents. A) Illustration of in-channel or in-canyon bypass on the basin floor, occurring when the slope gradient and grain size distribution of a flow favour erosion or non-deposition. B) An example of bypass in the Madeira turbidite system, where identifiable zones of bypass occur between depositional areas. Modified from Stevenson et al. (2015). C) Illustration of bypass on topographically complex slopes, where sand may pond in bathymetric lows and bypass slopes between. D) Sand thickness map of a series of salt-withdrawal minibasins in the Gulf of Mexico, showing bypass or reduced thickness between individual basins. Modified from Winker (1996). (E) Illustration of channel-lobe transition zone (CLTZ) near the mouth of a submarine canyon. F) Acoustic backscatter image showing possible CLTZ features in the Rosetta lobe of the Nile delta, as evidenced by differential backscatter at the ends of channels. Modified from Migeon et al. (2010) G) Shaded swath bathymetry image showing CLTZ-related scour features in the Rhone Fan, western Mediterranean, from Bonnel et al. (2005). H) Illustration of levee breaching and formation of a crevasse splay. I) Backscatter image of a deposit interpreted as a crevasse splay by Gardner (2017).

**Figure 5**: A) Schematic illustration of detachment by bottom currents, showing erosive moat and deposition of deepwater sandy contourites. B) Subsurface seismic amplitude image of kilometer-scale coarse-grained deposits (yellow and red colours) in avulsion lobes. Sands can be reworked by bottom currents from these lobes into separate sandbodies that are detached from the main lobate deposit. Modified from Viana (2008), as seen in Rebesco et al. (2014).

**Figure 6**: A) Illustration of the process of crosscutting of submarine channels in a fan system. Older channel (1) has been backfilled by sand but is being crosscut by erosional channel (2), which may be abandoned before backfilling occurs, leading to detachment of lobe (1) as the second, newer channel is filled by fines. B) Composite map of channels in the deepwater Amazon fan system and associated features. Instances of crosscutting highlighted in red; however, lithologies and depths of incision are unrecorded. Modified from Jegou et al. (2008), Pirmez et al. (1997), Flood et al. (1995), and Damuth

et al. (1988). C) Examples of presumably mud-filled channels in the subsurface that crosscut sandier channel or fan systems. Upper example (RMS amplitude extraction map and seismic line) modified from Mayall et al., (2006); location unrecorded. Lower example (AVO) from the North Atlantic Porcupine Basin (Providence Resources, 2016), showing bright-amplitude fan deposit cut by later mud-filled channel (white). Neither exact depths nor locations recorded for either example.

**Figure 7**: A) Schematic illustration of detachment processes and resulting depositional products due to mass-transport erosion. Pre-existing sandy channels and lobes are shown being decapitated by a large MTD originating from the upper slope. B) Example of the mechanism described in (A), near the Rosetta lobe of the Nile Delta and Fan in the eastern Mediterranean. Note defined channels terminating proximally into MTD. Modified from Garziglia et al. (2008).

**Figure 8**: A) Schematic illustration of translational slope failure processes, in which sandy units maintain their coherency (but may be deformed) while still moving downslope and becoming detached from the shelf and/or upper slope. B) Downdip seismic line showing failure of the Hikurangi Margin, New Zealand, and formation of the Tuaheni Landslide Complex. Unit II (orange) contains deformed, fining-upward sand beds, separated from the more proximal slope by the failure scarp shown here. Modified from Couvin et al., 2020. C) Subsurface horizon with RMS amplitude extraction, showing downslope slumping and detachment of Cretaceous sediments, offshore Ireland. Modified from Pedley et al., 2015.

**Figure 9**: Dip-oriented seismic line showing bottom-current erosion in the form of a slope-parallel moat in the Gulf of Cadiz, southern Portugal. Note also the presence of onlapping contourite deposits and interaction with turbidites, which frequently co-occur with deepwater bottom-current erosion. Modified from Hernández-Molina et al. (2010).

**Figure 10**: A) Schematic illustration of the various detachment processes discussed in this review, and their most likely locations on the slope. Not to scale. B) Table outlining primary (though not all) risks

for associated sand detachment for each process, and examples in the geologic record (subsurface or outcrop) where deposits affected by each process have been preserved.


## Acknowledgements

This research was funded by the Irish Centre for Research in Applied Geosciences (iCRAG) and University College Dublin. Additional support was provided during manuscript drafting by the United States Geological Survey. Any use of trade, firm, or product names is for descriptive purposes only and does not imply endorsement by the U.S. Government. The authors would like to thank Evan Bargnesi, Dr. Josh Long, Associate Editor Dr. Roberto Tinterri, and reviewers Dr. Javier Hernández-Molina and Dr. Fabiano Gamberi for helpful reviews and comments.


## References


Alleyne, K., Layne, L. & Soroush, M. (2018). Liza Field Development - The Guyanese Perspective. SPE-191239-MS.

Amante, C. and B.W. Eakins, 2009. ETOPO1 1 Arc-Minute Global Relief Model: Procedures, Data Sources and Analysis. NOAA Technical Memorandum NESDIS NGDC-24. National Geophysical Data Center, NOAA. doi:10.7289/V5C8276M

Amy, L. A. & Dorrell, R. M., in review. Equilibrium conditions for particle-laden flows: implications for near-equilibrium fields of sediment transport, bedform development, graded slope and palaeohydraulic interpretation. Submitted to Sedimentology.

Amy, L. A. (2019). A review of producing fields inferred to have upslope stratigraphically trapped turbidite reservoirs: Trapping styles (pure and combined), pinch-out formation, and depositional setting. AAPG Bulletin, 103(12), 2861-2889.

Babonneau, N., Savoye, B., Cremer, M., & Klein, B. (2002). Morphology and architecture of the present canyon and channel system of the Zaire deep-sea fan. Marine and Petroleum Geology, 19(4), 445-467.

Babonneau, N., Savoye, B., Cremer, M., & Bez, M. (2010). Sedimentary architecture in meanders of a submarine channel: detailed study of the present Congo turbidite channel (Zaiango project). Journal of Sedimentary Research, 80(10), 852-866.

Bain, H. A., & Hubbard, S. M. (2016). Stratigraphic evolution of a long-lived submarine channel system in the Late Cretaceous Nanaimo Group, British Columbia, Canada. Sedimentary Geology, 337, 113-132.

Biteau, J. J., Blaizot, M., Janodet, D., & de Clarens, P. (2014). Recent emerging paradigms in hydrocarbon exploration. First Break, 32(2).

Bonnel, C., Dennielou, B., Droz, L., Mulder, T., & Berné, S. (2005). Architecture and depositional pattern of the Rhône Neofan and recent gravity activity in the Gulf of Lions (western Mediterranean). Marine and Petroleum Geology, 22(6-7), 827-843.

Bouma, A. H. (2004). Key controls on the characteristics of turbidite systems. Geological Society, London, Special Publications, 222(1), 9-22.

Bozzano, G., Violante, R. A., & Cerredo, M. E. (2011). Middle slope contourite deposits and associated sedimentary facies off NE Argentina. Geo-Marine Letters, 31(5-6), 495-507.

Brackenridge, R. E., Stow, D. A., Hernández-Molina, F. J., Jones, C., Mena, A., Alejo, I., ... & Perez-Arlucea, M. (2018). Textural characteristics and facies of sand-rich contourite depositional systems. Sedimentology, 65(7), 2223-2252.

Brooks, H.L., Hodgson, D.M., Brunt, R.L., Peakall, J., Poyatos-Moré, M. and Flint, S.S., 2018. Disconnected submarine lobes as a record of stepped slope evolution over multiple sea-level cycles. Geosphere, 14(4), pp.1753-1779.

Bruhn, C.H. and Walker, R.G., 1995. High-resolution stratigraphy and sedimentary evolution of coarse-grained canyon-filling turbidites from the Upper Cretaceous transgressive megasequence, Campos Basin, offshore Brazil. Journal of Sedimentary Research, 65(4b), pp.426-442.

Bugge, T., Befring, S., Belderson, R. H., Eidvin, T., Jansen, E., Kenyon, N. H., ... & Sejrup, H. P. (1987). A giant three-stage submarine slide off Norway. Geo-marine letters, 7(4), 191-198.

Capella, W., Hernández-Molina, F.J., Flecker, R., Hilgen, F.J., Hssain, M., Kouwenhoven, T.J., Van Oorschot, M., Sierro, F.J., Stow, D.A.V., Trabucho-Alexandre, J. and Tulbure, M.A., 2017. Sandy contourite drift in the late Miocene Rifian Corridor (Morocco): Reconstruction of depositional environments in a foreland-basin seaway. Sedimentary Geology, 355, pp.31-57.

Cardona, S., Wood, L.J., Day-Stirrat, R.J., and Moscardelli, L., 2016, "Fabric development and pore-throat reduction in a mass-transport deposit in the Jubilee Gas Field, Eastern Gulf of Mexico: consequences for the sealing capacity of MTDs." In Submarine Mass Movements and their Consequences, pp. 27-37. Springer.

Cartigny, M.J., Postma, G., van den Berg, J.H. and Mastbergen, D.R., 2011. A comparative study of sediment waves and cyclic steps based on geometries, internal structures and numerical modeling. Marine Geology, 280(1-4), pp.40-56.

Chaytor, J. D., Uri, S., Solow, A. R., & Andrews, B. D. (2009). Size distribution of submarine landslides along the US Atlantic margin. Marine Geology, 264(1-2), 16-27.

Clark, J.D. and Pickering, K.T., 1996. Architectural elements and growth patterns of submarine channels: application to hydrocarbon exploration. AAPG bulletin, 80(2), pp.194-220.

Couvin, B., Georgiopoulou, A., Mountjoy, J.J., Amy, L., Crutchley, G.J., Brunet, M., Cardona, S., Gross, F., Böttner, C., Krastel, S. and Pecher, I., 2020. A new depositional model for the Tuaheni Landslide Complex, Hikurangi Margin, New Zealand. Geological Society, London, Special Publications, 500(1), pp.551-566.

Covault, J. A., Fildani, A., Romans, B. W., & McHargue, T. (2011). The natural range of submarine canyon-and-channel longitudinal profiles. Geosphere, 7(2), 313-332.

Covault, J. A., Shelef, E., Traer, M., Hubbard, S. M., Romans, B. W., & Fildani, A. (2012). Deep-water channel run-out length: Insights from seafloor geomorphology. Journal of Sedimentary Research, 82(1), 21-36.

Crisóstomo Figueroa A., McArthur A.D., Dorrell R.M., Amy L.A., McCaffrey W.D., 2020. A new modelling approach to sediment bypass prediction applied to the East Coast Basin, New Zealand. GSA Bulletin.

Cronin, B. T., Akhmetzhanov, A. M., Mazzini, A., Akhmanov, G., Ivanov, M., & Kenyon, N. H. (2005). Morphology, evolution and fill: Implications for sand and mud distribution in filling deep-water canyons and slope channel complexes. Sedimentary Geology, 179(1-2), 71-97.

Dailly, P., Henderson, T., Hudgens, E., Kanschat, K., & Lowry, P. (2013). Exploration for Cretaceous stratigraphic traps in the Gulf of Guinea, West Africa and the discovery of the Jubilee Field: a play opening discovery in the Tano Basin, Offshore Ghana. Geological Society, London, Special Publications, 369(1), 235-248.

Dailly, P., Henderson, T., Kanschat, K., Lowry, P., & Sills, S. (2017). The Jubilee Field, Ghana: Opening the Late Cretaceous Play in the West African Transform Margin.

Dakin, N., Pickering, K. T., Mohrig, D., & Bayliss, N. J. (2013). Channel-like features created by erosive submarine debris flows: field evidence from the Middle Eocene Ainsa Basin, Spanish Pyrenees. Marine and Petroleum Geology, 41, 62-71.

Dalla Valle, G., & Gamberi, F. (2011). Slope channel formation, evolution and backfilling in a wide shelf, passive continental margin (Northeastern Sardinia slope, Central Tyrrhenian Sea). Marine Geology, 286(1-4), 95-105.

Damuth, J.E., 2002. The Amazon-HARP fan model: facies distributions in mud-rich deep-sea fans based on systematic coring of architectural elements of Amazon Fan. Turbidite systems and deep sea fans of the Mediterranean and the Black Seas. CIESM Worksh, 17, pp.19-22.

Damuth, J.E., Flood, R.D., Kowsmann, R.O., Belderson, R.H., and Gorini, M.A., 1988. Anatomy and growth pattern of Amazon deep-sea fan as revealed by long-range side-scan sonar (GLORIA) and high-resolution seismic studies. Am. Assoc. Petrol. Geol. Bull., 72: 885-911.

de Castro, S., Hernandez-Molina, F.J., Rodríguez-Tovar, F.J., Llave, E., Ng, Z.L., Nishida, N. and Mena, A., 2020. Contourites and bottom current reworked sands: Bed facies model and implications. Marine Geology, 428, p.106267.

Defeo de Castro, R., 2014, Stratigraphic traps of turbidite fields in Campos Basin, Brazil (abs.): AAPG Geoscience Technology Workshop, Stratigraphic Traps and Play Concepts in Deepwater Settings, Rio de Janeiro, Brazil, May 14–15, 2014, accessed July 1, 2017

Deptuck, M. E., & Sylvester, Z. (2018). Submarine fans and their channels, levees, and lobes. In Submarine geomorphology (pp. 273-299). Springer, Cham.

Diaz, J., Weimer, P., Bouroullec, R., & Dorn, G. (2011). 3-D seismic stratigraphic interpretation of Quaternary mass-transport deposits in the Mensa and Thunder Horse intraslope basins, Mississippi Canyon, northern deep Gulf of Mexico, USA. Mass-Transport Deposits in Deepwater Settings. SEPM, Special Publications, 96, 127-149.

Dolson, J., He, Z., & Horn, B. W. (2018). Advances and perspectives on stratigraphic trap exploration-making the subtle trap obvious. In AAPG 2017 Middle East region geosciences technology workshop, stratigraphic traps of the Middle East, Muscat, Oman.

Providence Resources, (2016). Druid and Drombeg Technical Slide Pack. http://www.providenceresources.com/sites/default/files/Druid%20%26%20Drombeg%20-%20Introductory%20Presentation%20-%20April%202016_2.pdf. Accessed Sept. 21, 2020.

Ducassou, E., Migeon, S., Mulder, T., Murat, A., Capotondi, L., Bernasconi, S. M., & Mascle, J. (2009). Evolution of the Nile deep-sea turbidite system during the Late Quaternary: influence of climate change on fan sedimentation. Sedimentology, 56(7), 2061-2090.

Eggenhuisen, J.T., McCaffrey, W.D., Haughton, P.D.W., Butler, R.W.H., Moore, I., Jarvie, A. and Hakes, W.G., 2010. Reconstructing large-scale remobilisation of deep-water deposits and its impact on sand-body architecture from cored wells: The Lower Cretaceous Britannia Sandstone Formation, UK North Sea. Marine and Petroleum Geology, 27(7), pp.1595-1615.

Elliott, G. M., Shannon, P. M., Haughton, P. D., Praeg, D., & O'Reilly, B. (2006). Mid-to Late Cenozoic canyon development on the eastern margin of the Rockall Trough, offshore Ireland. Marine Geology, 229(3-4), 113-132.

Emmel, F. J., & Curray, J. R. (1983). The Bengal submarine fan, northeastern Indian Ocean. Geo-Marine Letters, 3(2-4), 119-124.

Faugères, J. C., & Mulder, T. (2011). Contour currents and contourite drifts. In Developments in Sedimentology (Vol. 63, pp. 149-214). Elsevier.

Faugères, J.C., Stow, D.A., Imbert, P. and Viana, A., 1999. Seismic features diagnostic of contourite drifts. Marine Geology, 162(1), pp.1-38.

Felix, M. and Peakall, J., 2006. Transformation of debris flows into turbidity currents: mechanisms inferred from laboratory experiments. Sedimentology, 53(1), pp.107-123.

Fildani, A., & Normark, W. R. (2004). Late Quaternary evolution of channel and lobe complexes of Monterey Fan. Marine Geology, 206(1-4), 199-223.

Fisher, R.V. (1983). Flow transformations in sediment gravity flows. Geology, 11(5), pp.273-274.

Flinch, J. F., Huedo, J. L., Verzi, H., González, H., Gerster, R., Mansaray, A. K., ... & Gerard, J. (2009). The Sierra Leone-Liberia Emerging Deepwater Province. In Proceedings of the AAPG Annual Convention (pp. 7-10).

Flood, R. D., D. J. W. Piper, A. Klaus, et al., (1995) Proceedings of the Ocean Drilling Program, Initial reports, Volume 155. 702 p.

Flood, R.D., Manley, P.L., Kowsmann, R.O., Appi, C.J. and Pirmez, C., 1991. Seismic facies and late Quaternary growth of Amazon submarine fan. In Seismic facies and sedimentary processes of submarine fans and turbidite systems (pp. 415-433). Springer, New York, NY.

Fonnesu, M., Palermo, D., Galbiati, M., Marchesini, M., Bonamini, E. and Bendias, D., 2020. A new world-class deep-water play-type, deposited by the syndepositional interaction of turbidity flows and bottom currents: The giant Eocene Coral Field in northern Mozambique. Marine and Petroleum Geology, 111, pp.179-201.

Frenz, M., Wynn, R.B., Georgiopoulou, A., Bender, V.B., Hough, G., Masson, D.G., Talling, P.J. and Cronin, B.T., 2009. Provenance and pathways of late Quaternary turbidites in the deep-water Agadir Basin, northwest African margin. International Journal of Earth Sciences, 98(4), pp.721-733.

Fryer, R.C. and Jobe, Z.R., 2019. Quantification of the bed-scale architecture of submarine depositional environments. The Depositional Record, 5(2), pp.192-211.

Fugelli, E. M., & Olsen, T. R. (2005). Risk assessment and play fairway analysis in frontier basins: Part 2—Examples from offshore mid-Norway. AAPG bulletin, 89(7), 883-896.

Gamberi, F. and Marani, M., 2007. Downstream evolution of the Stromboli slope valley (southeastern Tyrrhenian Sea). Marine Geology, 243(1-4), pp.180-199.

Gardner, J. V. (2017). The morphometry of the deep-water sinuous Mendocino Channel and the immediate environs, Northeastern Pacific Ocean. Geosciences, 7(4), 124.

Gardner, James V., Andrew A. Armstrong, and Brian R. Calder, 2016, Hatteras Transverse Canyon, Hatteras Outer Ridge and environs of the US Atlantic margin: A view from multibeam bathymetry and backscatter. Marine Geology 371: 18-32.

Gardner, M.H., Borer, J.M., and Bouma, A. H., 2000. Submarine channel architecture along a slope to basin profile, Brushy Canyon Formation,West Texas. In: Bouma, A.H., Stone, C.G. (Eds.), Fine-Grained Turbidite Systems. Memoir 72-American Association of Petroleum Geologists and Special Publication 68-SEPM, pp. 195e214.

Garziglia, S., Migeon, S., Ducassou, E., Loncke, L., & Mascle, J. (2008). Mass-transport deposits on the Rosetta province (NW Nile deep-sea turbidite system, Egyptian margin): characteristics, distribution, and potential causal processes. Marine Geology, 250(3-4), 180-198.

Georgiopoulou, A. and Cartwright, J.A., 2013. A critical test of the concept of submarine equilibrium profile. Marine and Petroleum Geology, 41, pp.35-47.

Georgiopoulou, A., Wynn, R. B., Masson, D. G., & Frenz, M. (2009). Linked turbidite–debrite resulting from recent Sahara Slide headwall reactivation. Marine and Petroleum Geology, 26(10), 2021-2031.

Georgiopoulou, A., Masson, D. G., Wynn, R. B., & Krastel, S. (2010). Sahara Slide: Age, initiation, and processes of a giant submarine slide. Geochemistry, Geophysics, Geosystems, 11(7).

Godo, T. J. (2006). Identification of stratigraphic traps with subtle seismic amplitude effects in Miocene channel/levee sand systems, NE Gulf of Mexico. Geological Society, London, Special Publications, 254(1), 127-151.

Hadler-Jacobsen, F., Johannessen, E. P., Ashton, N., Henriksen, S., Johnson S. D., and Kristensen, J. B., 2005, Submarine fan morphology and lithology distribution: a predictable function of sediment delivery, gross shelf-to-basin relief, slope gradient and basin topography. Petroleum Geology Conference series 2005, v.6; p. 1121-1145. doi: 10.1144/0061121

Haflidason, H., Sejrup, H. P., Nygård, A., Mienert, J., Bryn, P., Lien, R., ... & Masson, D. (2004). The Storegga Slide: architecture, geometry and slide development. Marine geology, 213(1-4), 201-234.

Hansen, L. A. S., Hodgson, D. M., Pontén, A., Bell, D., & Flint, S. (2019). Quantification of basin-floor fan pinchouts: examples from the Karoo Basin, South Africa. Frontiers in Earth Science, 7.

He, Y., Zhong, G., Wang, L., & Kuang, Z. (2014). Characteristics and occurrence of submarine canyon-associated landslides in the middle of the northern continental slope, South China Sea. Marine and Petroleum Geology, 57, 546-560.

Henstra, G.A., Grundvåg, S.A., Johannessen, E.P., Kristensen, T.B., Midtkandal, I., Nystuen, J.P., Rotevatn, A., Surlyk, F., Sæther, T. and Windelstad, J., 2016. Depositional processes and stratigraphic architecture within a coarse-grained rift-margin turbidite system: The Wollaston Forland Group, east Greenland. Marine and Petroleum Geology, 76, pp.187-209.

Hernández-Molina, J., Llave, E., Somoza, L., Fernández-Puga, M. C., Maestro, A., León, R., ... & Fernández-Salas, L. M. (2003). Looking for clues to paleoceanographic imprints: a diagnosis of the Gulf of Cadiz contourite depositional systems. Geology, 31(1), 19-22.

Hernández-Molina, F. J., Llave, E., & Stow, D. A. V. (2008). Continental slope contourites. Developments in sedimentology, 60, 379-408.

Hernández-Molina, F. J., Paterlini, M., Violante, R., Marshall, P., de Isasi, M., Somoza, L., & Rebesco, M. (2009). Contourite depositional system on the Argentine Slope: An exceptional record of the influence of Antarctic water masses. Geology, 37(6), 507-510.

Hernández-Molina, F.J., Paterlini, M., Somoza, L., Violante, R., Arecco, M.A., De Isasi, M., Rebesco, M., Uenzelmann-Neben, G., Neben, S. and Marshall, P., 2010. Giant mounded drifts in the Argentine Continental Margin: origins, and global implications for the history of thermohaline circulation. Marine and Petroleum Geology, 27(7), pp.1508-1530.

Hernández-Molina, F. J., Sierro, F. J., Llave, E., Roque, C., Stow, D. A. V., Williams, T., ... & Rosales, C. (2016). Evolution of the gulf of Cadiz margin and southwest Portugal contourite depositional system: Tectonic, sedimentary and paleoceanographic implications from IODP expedition 339. Marine Geology, 377, 7-39.

Hernández-Molina, F.J., Campbell, S., Badalini, G., Thompson, P., Walker, R., Soto, M., Conti, B., Preu, B., Thieblemont, A., Hyslop, L., Miramontes, E., Morales, E. 2018. Large bedforms on contourite terraces: Sedimentary and conceptual implications. Geology, 46 (1), 27-30.

Hofstra, M., Peakall, J., Hodgson, D.M. and Stevenson, C.J., 2018. Architecture and morphodynamics of subcritical sediment waves in an ancient channel–lobe transition zone. Sedimentology, 65(7), pp.2339-2367.

Horseman, C., A. Ross, and S. Cannon, (2014), The discovery and appraisal of Glenlivet: A West of Shetlands success story: Geological Society, London, Special Publications 2014, v. 397, p. 131–144 https://www.ogj.com/exploration-development/discoveries/article/17232594/study-questions-predrill-risks-associated-with-stratigraphic-traps. Accessed March 11th, 2020.

Janocko, M. N. W. H. S. W. M., Nemec, W., Henriksen, S., & Warchoł, M. (2013). The diversity of deep-water sinuous channel belts and slope valley-fill complexes. Marine and Petroleum Geology, 41, 7-34.

Jegou, I., Savoye, B., Pirmez, C., & Droz, L. (2008). Channel-mouth lobe complex of the recent Amazon Fan: the missing piece. Marine Geology, 252(1-2), 62-77.

Kastens, K. A. (1984). Earthquakes as a triggering mechanism for debris flows and turbidites on the Calabrian Ridge. Marine Geology, 55(1-2), 13-33.

Kelly, J., and H. Doust, (2016), Exploration for Late Cretaceous turbidites in the equatorial African and northeast South American margins: Netherlands Journal of Geosciences, v. 95, no. 4, p. 393–403

Klaucke, I., Savoye, B. and Cochonat, P., 2000. Patterns and processes of sediment dispersal on the continental slope off Nice, SE France. Marine Geology, 162(2-4), pp.405-422.

Kneller, B. (2003). The influence of flow parameters on turbidite slope channel architecture. Marine and Petroleum Geology, 20(6-8), 901-910.

Komar, P. D. (1971). The mechanics of sand transport on beaches. Journal of Geophysical Research, 76(3), 713-721.

Krastel, S., Wynn, R.B., Georgiopoulou, A., Geersen, J., Henrich, R., Meyer, M. and Schwenk, T., 2012. Large-scale mass wasting on the Northwest African continental margin: Some general implications for mass wasting on passive continental margins. In Submarine mass movements and their consequences (pp. 189-199). Springer, Dordrecht.

Lewis, K.B. and Kohn, B.P., 1973. Ashes, turbidites, and rates of sedimentation on the continental slope off Hawkes Bay. New Zealand journal of geology and geophysics, 16(3), pp.439-454.

Lewis, K.B., 1980. Quaternary sedimentation on the Hikurangi oblique-subduction and transform margin, New Zealand. In Sedimentation in oblique-slip mobile zones (Vol. 4, pp. 171-189).

Llave, E., Hernández-Molina, F.J., Somoza, L., Stow, D.A.V., Díaz del Río, V., 2007. Quaternary evolution of the contourite depositional system in the gulf of Cadiz. In: Viana, A., Rebesco,M. (Eds.), Economic and Paleoceanographic Importance of Contourites. Geol Soc London Sp Publ 276, pp. 49–79.

Iacono, C.L., Sulli, A., Agate, M., Presti, V.L., Pepe, F. and Catalano, R., 2011. Submarine canyon morphologies in the Gulf of Palermo (Southern Tyrrhenian Sea) and possible implications for geo-hazard. Marine Geophysical Research, 32(1-2), p.127.

Loizou, N. (2014). Success in exploring for reliable, robust Paleocene traps west of Shetland. Geological Society, London, Special Publications, 397(1), 59-79.

Lowe, D. R., Graham, S. A., Malkowski, M. A., & Das, B. (2019). The role of avulsion and splay development in deep-water channel systems: Sedimentology, architecture, and evolution of the deep-water Pliocene Godavari “A” channel complex, India. Marine and Petroleum Geology, 105, 81-99.

Macdonald, H. A., Wynn, R. B., Huvenne, V. A., Peakall, J., Masson, D. G., Weaver, P. P., & McPhail, S. D. (2011). New insights into the morphology, fill, and remarkable longevity (> 0.2 my) of modern deep-water erosional scours along the northeast Atlantic margin. Geosphere, 7(4), 845-867.

MacPherson, B.A., 1978. Sedimentation and trapping mechanism in upper Miocene Stevens and older turbidite fans of southeastern San Joaquin Valley, California. AAPG Bulletin, 62(11), pp.2243-2274.

Manson, S. (2009). Avulsion process: stratigraphic and lithologic records-Application to the Amazon and Zaïre turbidite systems (Doctoral dissertation).

Masson, D.G., Van Niel, B. and Weaver, P.P.E., 1997. Flow processes and sediment deformation in the Canary debris flow on the NW African continental rise. Sedimentary Geology, 110(3-4), pp.163-179.

Mathieu, C. J. (2018). Exploration well failures from the UK North Sea. In Geological Society, London, Petroleum Geology Conference series (Vol. 8, No. 1, pp. 267-272). Geological Society of London.

Mayall, M., Jones, E., & Casey, M. (2006). Turbidite channel reservoirs—Key elements in facies prediction and effective development. Marine and Petroleum Geology, 23(8), 821-841.

McAdoo, B. G., Pratson, L. F., & Orange, D. L. (2000). Submarine landslide geomorphology, US continental slope. Marine Geology, 169(1-2), 103-136.

McArthur, A.D. and McCaffrey, W.D., 2019. Sedimentary architecture of detached deep-marine canyons: Examples from the East Coast Basin of New Zealand. Sedimentology, 66(3), pp.1067-1101.

Myers, K., 2020, Why excelling in stratigraphic trap exploration is now the key to top quartile performance. https://www.westwoodenergy.com/news/westwood-insight/why-excelling-in-stratigraphic-trap-exploration-is-now-the-key-to-top-quartile-performance. Accessed September 17th, 2020.

Migeon, S., Savoye, B. and Faugeres, J.C., 2000. Quaternary development of migrating sediment waves in the Var deep-sea fan: distribution, growth pattern, and implication for levee evolution. Sedimentary Geology, 133(3-4), pp.265-293.

Migeon, S., Ducassou, E., Le Gonidec, Y., Rouillard, P., Mascle, J., & Revel-Rolland, M. (2010). Lobe construction and sand/mud segregation by turbidity currents and debris flows on the western Nile deep-sea fan (Eastern Mediterranean). Sedimentary Geology, 229(3), 124-143.

Mohrig, D. and Marr, J.G., 2003. Constraining the efficiency of turbidity current generation from submarine debris flows and slides using laboratory experiments. Marine and Petroleum Geology, 20(6-8), pp.883-899.

Moscardelli, L., Wood, L., & Mann, P. (2006). Mass-transport complexes and associated processes in the offshore area of Trinidad and Venezuela. AAPG bulletin, 90(7), 1059-1088.

Mountjoy, J.J., Howarth, J.D., Orpin, A.R., Barnes, P.M., Bowden, D.A., Rowden, A.A., Schimel, A.C., Holden, C., Horgan, H.J., Nodder, S.D. and Patton, J.R., 2018. Earthquakes drive large-scale submarine canyon development and sediment supply to deep-ocean basins. Science advances, 4(3), eaar3748, p. 1-8..

Mutti, E., & Normark, W. R. (1987). Comparing examples of modern and ancient turbidite systems: problems and concepts. In Marine clastic sedimentology (pp. 1-38). Springer, Dordrecht.

Mutti, E., 1977. Distinctive thin-bedded turbidite facies and related depositional environments in the Eocene Hecho Group (South-central Pyrenees, Spain). Sedimentology, 24(1), pp.107-131.

Mutti, E. (1985). Turbidite systems and their relations to depositional sequences. In Provenance of arenites (pp. 65-93). Springer, Dordrecht.

Mutti, E. (1992). Turbidite sandstones. Agip, Istituto di geologia, Università di Parma.

National Oceanic and Atmospheric Administration (NOAA), https://www.ngdc.noaa.gov/mgg/topo/pictures/GLOBALeb10colshade.jpg

Nelson, C. H., Baraza, J., & Maldonado, A. (1993). Mediterranean undercurrent sandy contourites, Gulf of Cadiz, Spain. Sedimentary Geology, 82(1-4), 103-131.

Normark, W. R. (1978). Fan valleys, channels, and depositional lobes on modern submarine fans: characters for recognition of sandy turbidite environments. AAPG Bulletin, 62(6), 912-931.

Normark, W. R., & Piper, D. J. (1991). Initiation processes and flow evolution of turbidity currents: implications for the depositional record.

Palanques, A., Kenyon, N. H., Alonso, B., & Limonov, A. (1995). Erosional and depositional patterns in the Valencia Channel mouth: an example of a modern channel-lobe transition zone. Marine Geophysical Researches, 17(6), 503-517.

Paull, C. K., Mitts, P., Ussler III, W., Keaten, R., & Greene, H. G. (2005). Trail of sand in upper Monterey Canyon: offshore California. Geological Society of America Bulletin, 117(9-10), 1134-1145.

Pecher, I.A., Barnes, P.M., Levay, L.J. and Expedition 372 Scientists 2018. Expedition 372 Preliminary Report Creeping Gas Hydrate Slides and Hikurangi LWD, November 2017.

Pedley, P., Spear, G., and Byrne, K. (2015). Ireland: South Porcupine Basin. GeoExPro 12(3) 38-40.

Pettingill, H. S. (1998). Turbidite plays' immaturity means big potential remains. Oil and Gas Journal, 96(40).

Picot, M., Droz, L., Marsset, T., Dennielou, B., & Bez, M. (2016). Controls on turbidite sedimentation: insights from a quantitative approach of submarine channel and lobe architecture (Late Quaternary Congo Fan). Marine and Petroleum Geology, 72, 423-446.

Piper, D. J., & Normark, W. R. (1983). Turbidite depositional patterns and flow characteristics, Navy submarine fan, California Borderland. Sedimentology, 30(5), 681-694.

Pirmez, C., Hiscou, R.N. and Kronen, J.K., 1997. Sandy turbidite successions at the base of channel-levee systems of the Amazon Fan revealed by FMS logs and cores: Unraveling the facies architecture of large submarine fans. In Proceedings-Ocean Drilling Program Scientific Results (pp. 7-34). National science foundation.

Pirmez, C., & Flood, R. D. (1995). Morphology and structure of Amazon Channel. In Proceedings of the Ocean Drilling Program. Part A, Initial report (Vol. 155, pp. 23-45).

Pohl, F., Eggenhuisen, J. T., Tilston, M., & Cartigny, M. J. B. (2019). New flow relaxation mechanism explains scour fields at the end of submarine channels. Nature communications, 10(1), 1-8.

Posamentier, H.W., Davies, R.J., Cartwright, J.A., Wood, L.J., 2007. Seismic geomorphol-ogy—an overview. In: Davies, R.J., Posamentier, H.W., Wood, L.J., Cartwright, J.A.(Eds.), Seismic Geomorphology: Applications to Hydrocarbon Exploration and Production. Special Publication. Geological Society of London, pp. 1–14.

Postma, G., Hoyal, D. C., Abreu, V., Cartigny, M. J., Demko, T., Fedele, J. J., ... & Pederson, K. H. (2016). Morphodynamics of supercritical turbidity currents in the channel-lobe transition zone. In Submarine Mass Movements and their Consequences (pp. 469-478). Springer, Cham.

Postma, G., Hoyal, D.C., Abreu, V., Cartigny, M.J., Demko, T., Fedele, J.J., Kleverlaan, K. and Pederson, K.H., 2016. Morphodynamics of supercritical turbidity currents in the channel-lobe transition zone. In Submarine Mass Movements and their Consequences (pp. 469-478). Springer, Cham.

Postma, G., Kleverlaan, K., & Cartigny, M. J. (2014). Recognition of cyclic steps in sandy and gravelly turbidite sequences, and consequences for the Bouma facies model. Sedimentology, 61(7), 2268-2290.

Prather, B. E. (2003). Controls on reservoir distribution, architecture and stratigraphic trapping in slope settings. Marine and Petroleum Geology, 20(6-8), 529-545.

Reading, H. G., & Richards, M. (1994). Turbidite systems in deep-water basin margins classified by grain size and feeder system. AAPG bulletin, 78(5), 792-822.

Rebesco, M., Hernández-Molina, F. J., Van Rooij, D., & Wåhlin, A. (2014). Contourites and associated sediments controlled by deep-water circulation processes: state-of-the-art and future considerations. Marine Geology, 352, 111-154.

Samuel, A., Kneller, B., Raslan, S., Sharp, A., & Parsons, C. (2003). Prolific deep-marine slope channels of the Nile Delta, Egypt. AAPG bulletin, 87(4), 541-560.

Schwenk, T., & Spieß, V. (2009). Architecture and stratigraphy of the Bengal Fan as response to tectonic and climate revealed from high-resolution seismic data. External Controls on Deep-Water Depositional Systems. Special Publication-SEPM (Society of Sedimentary Geologists), 92, 107-131.

Shanmugam, G., Spalding, T. D., & Rofheart, D. H. (1993). Process sedimentology and reservoir quality of deep-marine bottom-current reworked sands (sandy contourites): an example from the Gulf of Mexico. AAPG Bulletin, 77(7), 1241-1259.

Smith, R.U., Lomas, S.A. and Joseph, P., 2004. Silled sub-basins to connected tortuous corridors: Sediment distribution systems on topographically complex sub-aqueous slopes. Special Publication-Geological Society of London, 222, pp.23-44.

Sobiesiak, M. S., Kneller, B., Alsop, G. I., & Milana, J. P. (2018). Styles of basal interaction beneath mass transport deposits. Marine and Petroleum Geology, 98, 629-639.

Stelting, C. E., L. Droz, A. H. Bouma, J. M. Coleman, M. Cremer, A. W. Meyer, W. R. Normark, S. O'Connell, and D. A. V. Stow, 1986, Late Pleistocene seismic stratigraphy of the Mississippi Fan, in A. H. Bouma, J. M. Coleman, and A. W. Meyer, eds., Initial reports of DSDP Leg 96 : U.S. Government Printing Office, p. 437–456.

Stevenson, C. J., Jackson, C. A. L., Hodgson, D. M., Hubbard, S. M., & Eggenhuisen, J. T. (2015). Deep-Water Sediment Bypass. Journal of Sedimentary Research, 85(9), 1058-1081.

Stirling, E. J., Fugelli, E. M., & Thompson, M. (2018). The edges of the wedges: a systematic approach to trap definition and risking for stratigraphic, combination and sub-unconformity traps. In: Geological Society, London, Petroleum Geology Conference series (Vol. 8, No. 1, pp. 273-286). Geological Society of London.

Stow, D. A. V., S. Hunter, D. Wilkinson, and F. J. Hernández-Molina. "The nature of contourite deposition." Developments in sedimentology 60 (2008): 143-156.

Straccia, J. R., & Prather, B. E. (1999). Stratigraphic traps in deep-water turbidite reservoirs at the base of depositional slope. In Society of Petroleum Engineers, Offshore Europe Conference, SPE (Vol. 56894).

Talling, P.J., 2014. On the triggers, resulting flow types and frequencies of subaqueous sediment density flows in different settings. Marine Geology, 352, pp.155-182.

Twichell, D. C., Schwab, W. C., Kenyon, N. H., & Lee, H. J. (1996). Breaching the levee of a channel on the Mississippi Fan: Chapter 5. In: Geology of the United States' Seafloor: The View from GLORIA, Cambridge University Press, 85-96.

Urlaub, M., Talling, P. J., Zervos, A., & Masson, D. (2015). What causes large submarine landslides on low gradient (< 2°) continental slopes with slow (~ 0.15 m/kyr) sediment accumulation?. Journal of Geophysical Research: Solid Earth, 120(10), 6722-6739.

Van der Merwe, W. C., Hodgson, D. M., Brunt, R. L., & Flint, S. S. (2014). Depositional architecture of sand-attached and sand-detached channel-lobe transition zones on an exhumed stepped slope mapped over a 2500 km2 area. Geosphere, 10(6), 1076-1093.

Vendettuoli, D., Clare, M. A., Clarke, J. H., Vellinga, A., Hizzet, J., Hage, S., ... & Stacey, C. (2019). Daily bathymetric surveys document how stratigraphy is built and its extreme incompleteness in submarine channels. Earth and Planetary Science Letters, 515, 231-247.

Viana, A. R. (2008). Economic relevance of contourites. Developments in Sedimentology, 60, 491-510.

Weaver, P. P. E., and J. Thomson (1993), Calculating erosion by deep-sea turbidity currents during initiation and flow, Nature, 364(6433),136–138.

Weaver, P.P.E., Masson, D.G., Gunn, D.E., Kidd, R.B., Rothwell, R.G. and Maddison, D.A., 1995. Sediment mass wasting in the Canary Basin. In Atlas of Deep Water Environments (pp. 287-296). Springer, Dordrecht.

Weimer, P., & Pettingill, H. S. (2007). Deep-water exploration and production: A global overview. Atlas of deep-water outcrops: AAPG Studies in Geology, 56.

Winker, C. D. (1996). High-resolution seismic stratigraphy of a late Pleistocene submarine fan ponded by salt-withdrawal mini-basins on the Gulf of Mexico continental slope. In Offshore Technology Conference. Offshore Technology Conference.

Wynn, R. B., Kenyon, N. H., Masson, D. G., Stow, D. A., & Weaver, P. P. (2002a). Characterization and recognition of deep-water channel-lobe transition zones. AAPG bulletin, 86(8), 1441-1462.

Wynn, R. B., Piper, D. J., & Gee, M. J. (2002b). Generation and migration of coarse-grained sediment waves in turbidity current channels and channel–lobe transition zones. Marine Geology, 192(1-3), 59-78.

Zanella, E., and Collard J., (2018). Study questions predrill risks associated with stratigraphic traps. Oil and Gas Journal, 116, (4), 36-39.

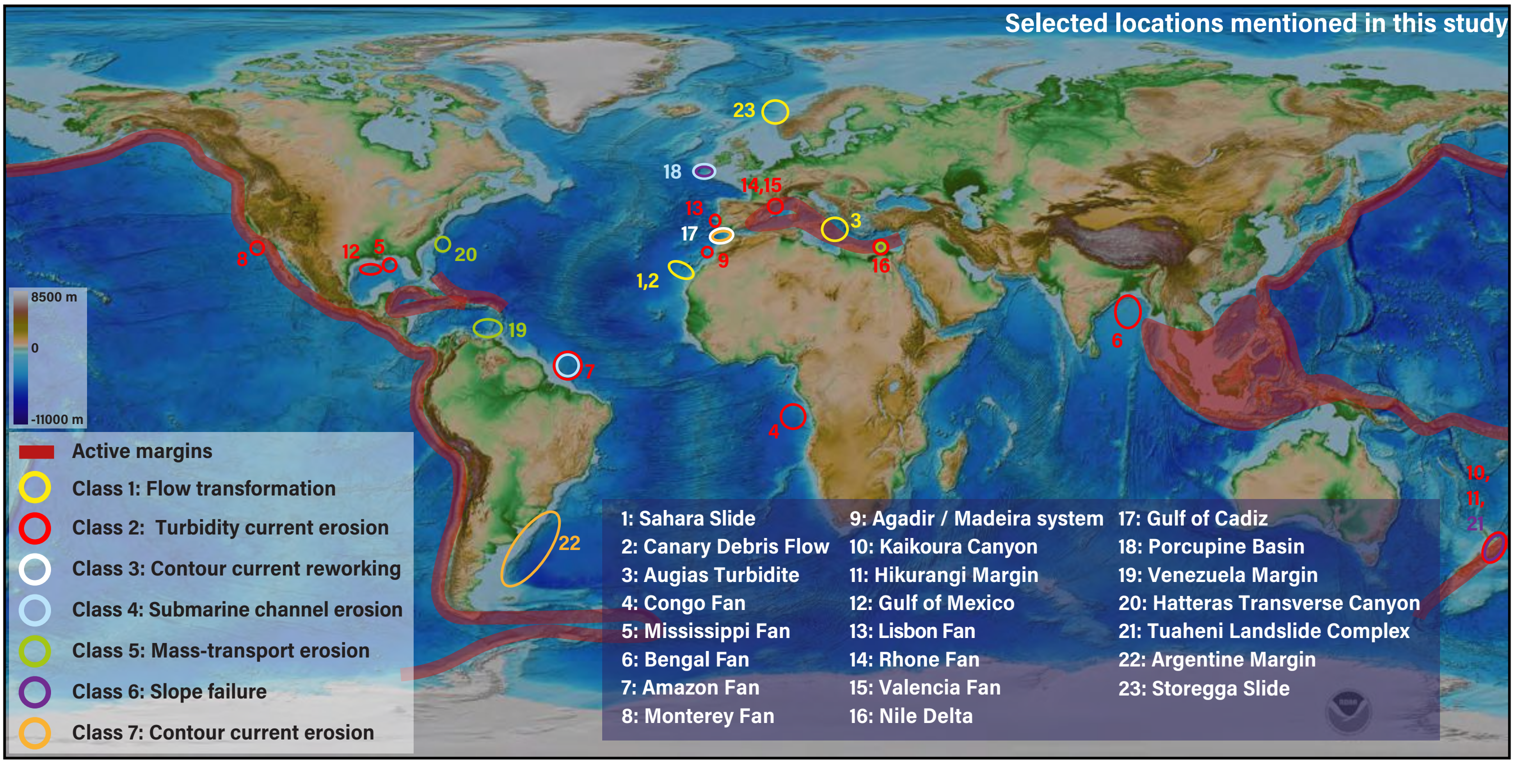


https://www.ngdc.noaa.gov/mgg/topo/pictures/GLOBALeb10colshade.jpg

| Timing | Category | | Process | | | General Description | Schematic |
|---|---|---|---|---|---|---|---|
| ***Syndepositional Detachment*** | Class 1 | | Gravitational | | Debris flow transformation | Lateral facies change into poorly sorted deposits or sand body onlap onto failure scar | 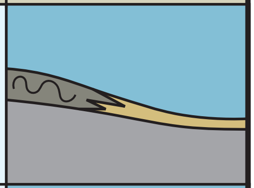 |
| | Class 2 | 2A | Gravitational | Turbidity current erosion and bypass | Channel or canyon bypass | Sand body pinchout against a bypass surface | 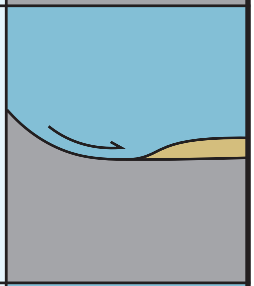 |
| | | 2B | | | Bypass due to slope topography | | |
| | | 2C | | | Channel-lobe transition zones | | |
| | | 2D | | | Crevassing | | |
| | Class 3 | | Bottom current | | Bottom-current reworking | Redistribution of sands into isolated bodies by deepwater currents | 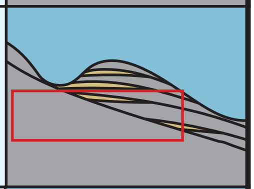 |
| ***Postdepositional Detachment*** | Class 4 | | Gravitational | | Submarine channel erosion | Sand body truncated by later channel incision | 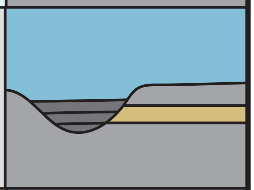 |
| | Class 5 | | Gravitational | | Mass-transport erosion | Sand body truncated by erosion at the base of a subsequent mass-transport deposit | 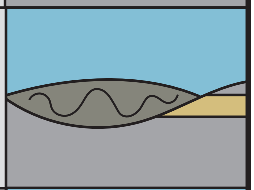 |
| | Class 6 | | Gravitational | | Translational slope failure | Preexisting sand deposit detached by sliding or slumping, but maintaining original integrity | 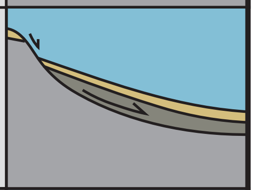 |
| | Class 7 | | Bottom current | | Bottom-current erosion | Erosion and disconnection of sands by deepwater currents | 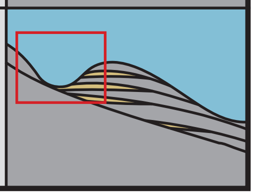 |

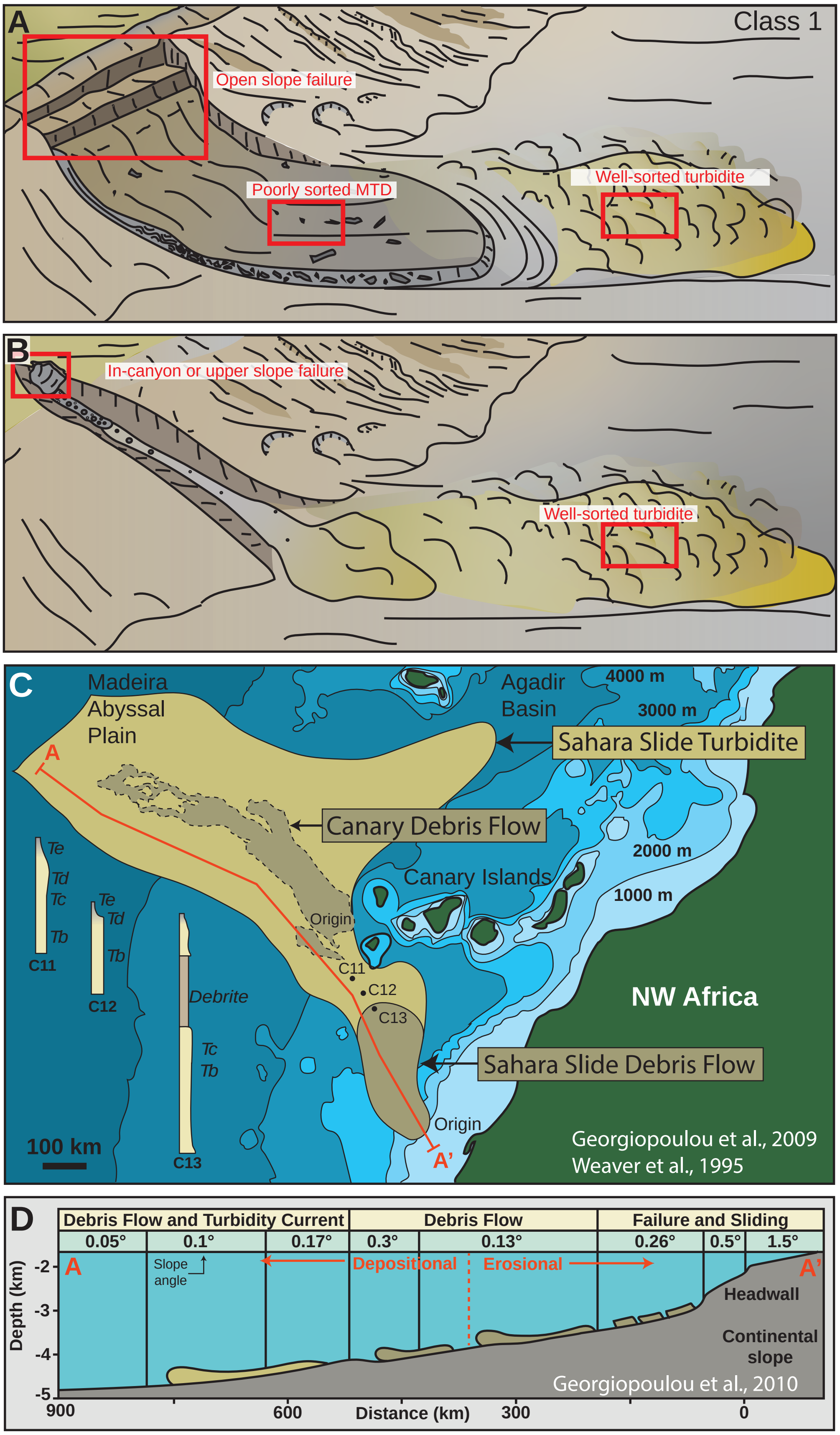

A
Class 1
Open slope failure
Poorly sorted MTD
Well-sorted turbidite
B
In-canyon or upper slope failure
Well-sorted turbidite
C
Madeira
Abyssal
Plain
Agadir
Basin
4000 m
3000 m
Sahara Slide Turbidite
Canary Debris Flow
Canary Islands
2000 m
1000 m
Origin
C11
C12
C13
Te
Td
Tc
Tb
Debrite
NW Africa
Sahara Slide Debris Flow
Origin
A
A'
100 km
Georgiopoulou et al., 2009
Weaver et al., 1995
D
Debris Flow and Turbidity Current
Debris Flow
Failure and Sliding
0.05°
0.1°
0.17°
0.3°
0.13°
0.26°
0.5°
1.5°
Slope angle
Depositional
Erosional
Headwall
Continental slope
Depth (km)
-2
-3
-4
-5
900
600
Distance (km)
300
0
Georgiopoulou et al., 2010

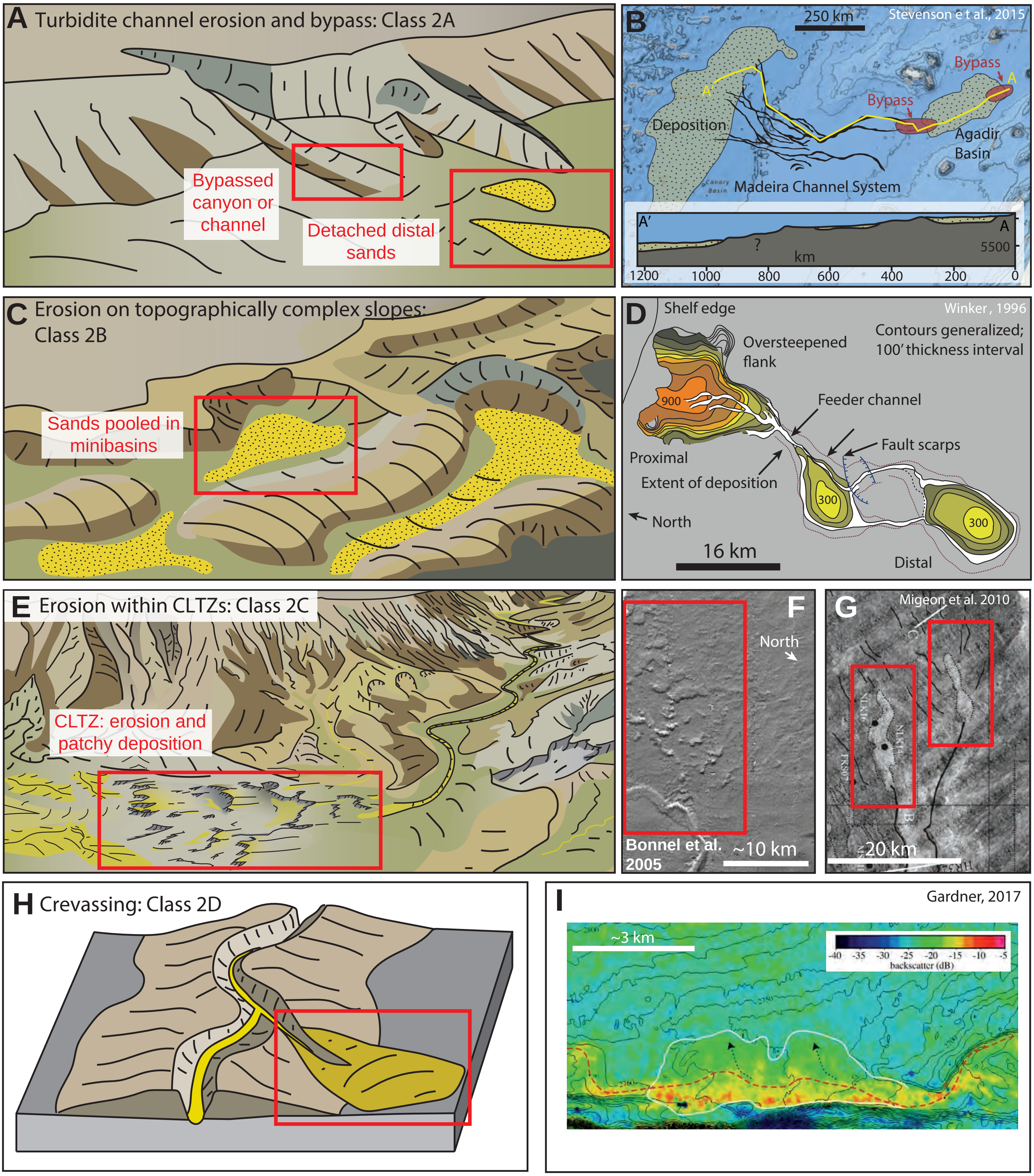

A Turbidite channel erosion and bypass: Class 2A
Bypassed canyon or channel
Detached distal sands
B
250 km
Stevenson et al., 2015
Bypass
Bypass
A
A'
Deposition
Agadir Basin
Madeira Channel System
A'
A
?
km
5500
1200
1000
800
600
400
200
0
C Erosion on topographically complex slopes: Class 2B
Sands pooled in minibasins
D
Shelf edge
Winker, 1996
Oversteepened flank
Contours generalized; 100' thickness interval
900
Feeder channel
Fault scarps
Proximal
Extent of deposition
300
300
North
16 km
Distal
E Erosion within CLTZs: Class 2C
CLTZ: erosion and patchy deposition
F
North
Bonnel et al. 2005
~10 km
G
Migeon et al. 2010
20 km
H Crevassing: Class 2D
I
Gardner, 2017
~3 km
-40
-35
-30
-25
-20
-15
-10
-5
backscatter (dB)

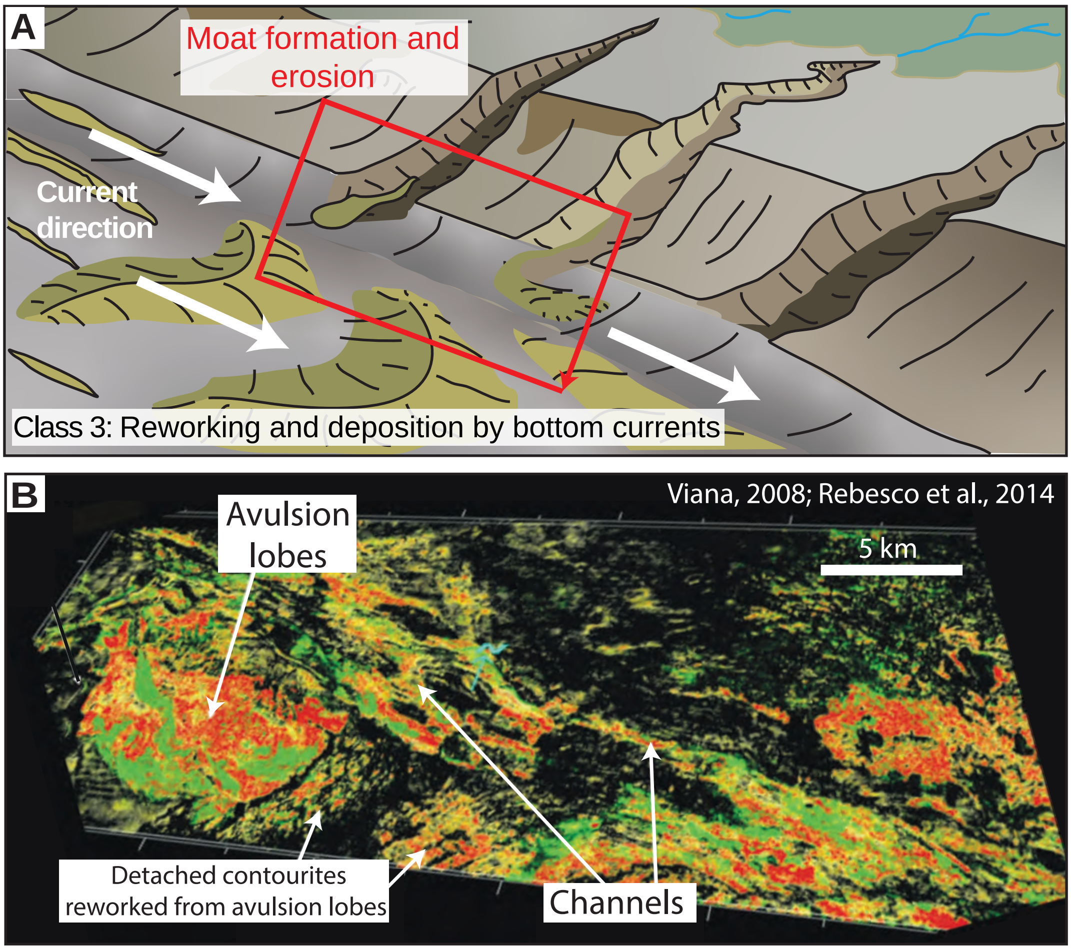
A
Moat formation and erosion
Current direction
Class 3: Reworking and deposition by bottom currents
B
Viana, 2008; Rebesco et al., 2014
Avulsion lobes
5 km
Detached contourites reworked from avulsion lobes
Channels

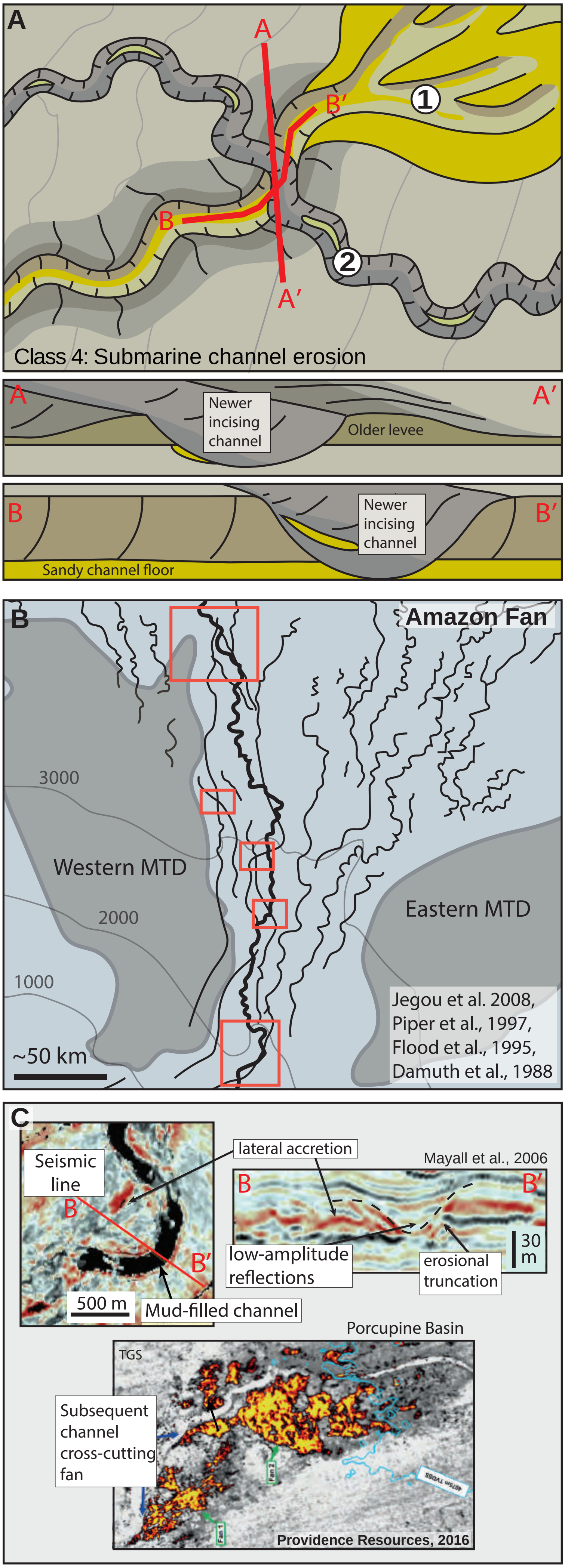

A
A
B′
1
B
2
A′
Class 4: Submarine channel erosion
A
Newer incising channel
Older levee
A′
B
Newer incising channel
B′
Sandy channel floor
B
Amazon Fan
3000
Western MTD
2000
Eastern MTD
1000
~50 km
Jegou et al. 2008, Piper et al., 1997, Flood et al., 1995, Damuth et al., 1988
C
Seismic line
B
B′
lateral accretion
Mayall et al., 2006
B
B′
30 m
low-amplitude reflections
erosional truncation
500 m
Mud-filled channel
Porcupine Basin
TGS
Subsequent channel cross-cutting fan
Providence Resources, 2016

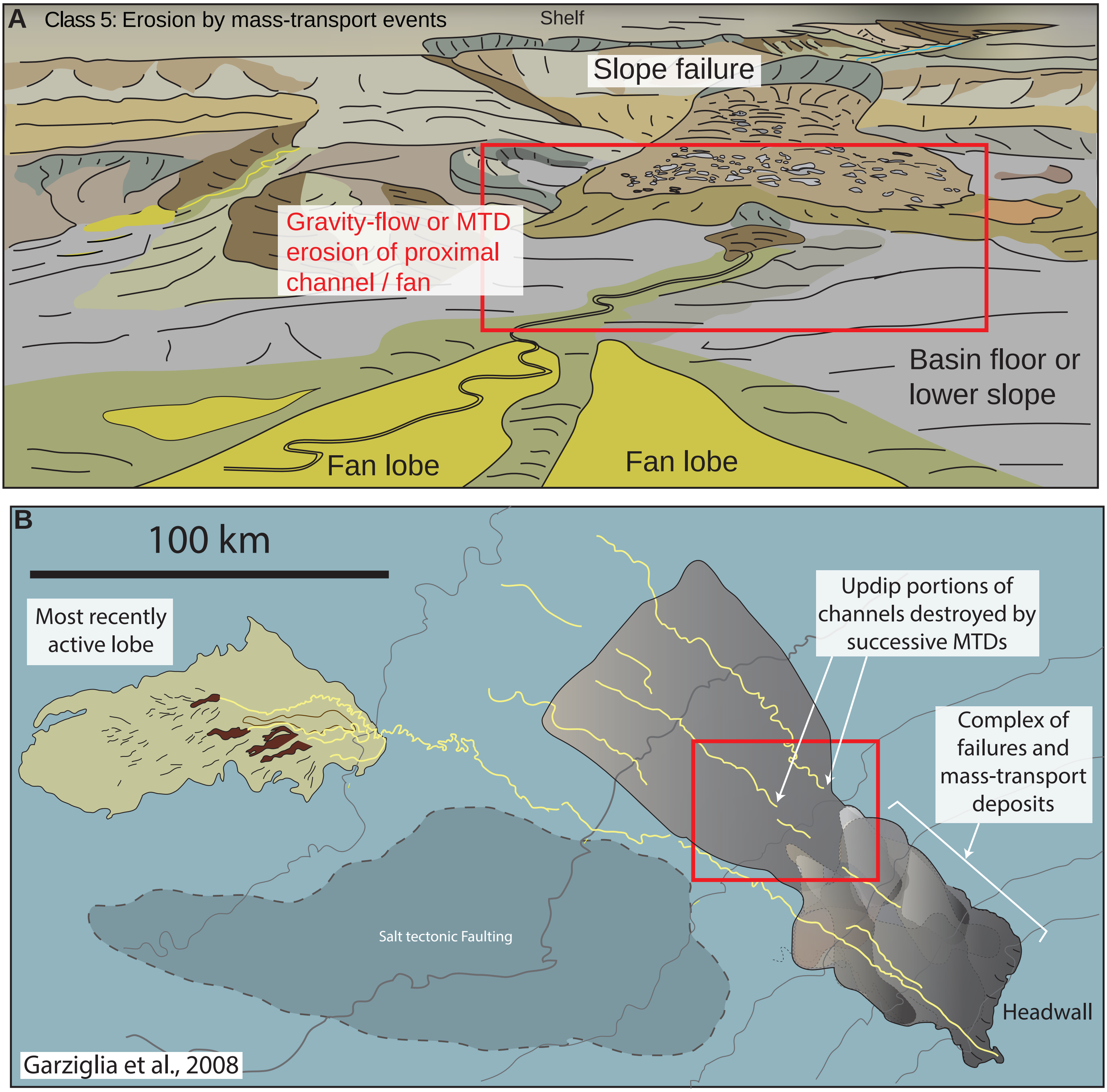
A
Class 5: Erosion by mass-transport events
Shelf
Slope failure
Gravity-flow or MTD erosion of proximal channel / fan
Basin floor or lower slope
Fan lobe
Fan lobe
B
100 km
Most recently active lobe
Updip portions of channels destroyed by successive MTDs
Complex of failures and mass-transport deposits
Salt tectonic Faulting
Headwall
Garziglia et al., 2008

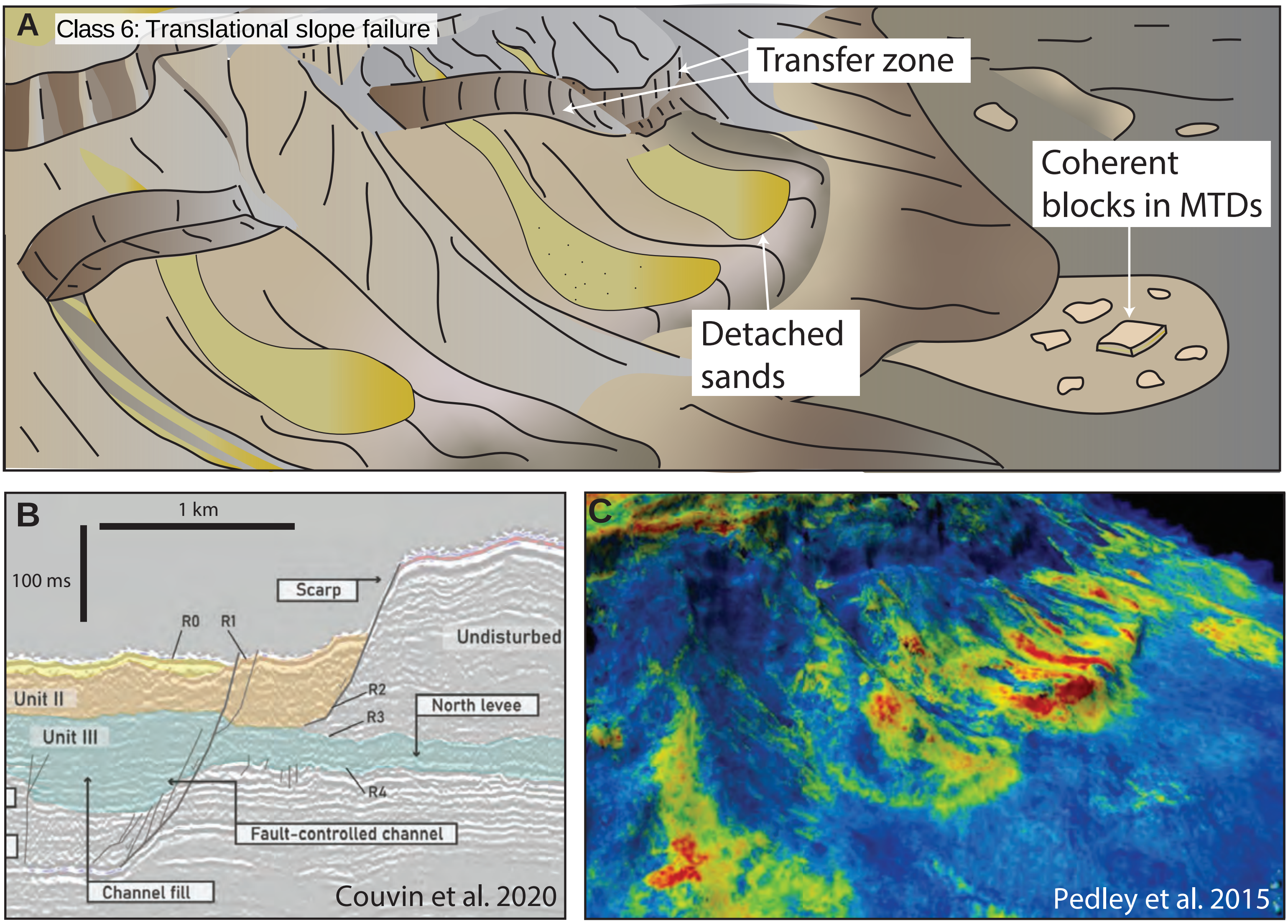
A
Class 6: Translational slope failure
Transfer zone
Coherent blocks in MTDs
Detached sands
B
1 km
100 ms
Scarp
Undisturbed
R0
R1
R2
R3
R4
Unit II
Unit III
North levee
Fault-controlled channel
Channel fill
Couvin et al. 2020
C
Pedley et al. 2015

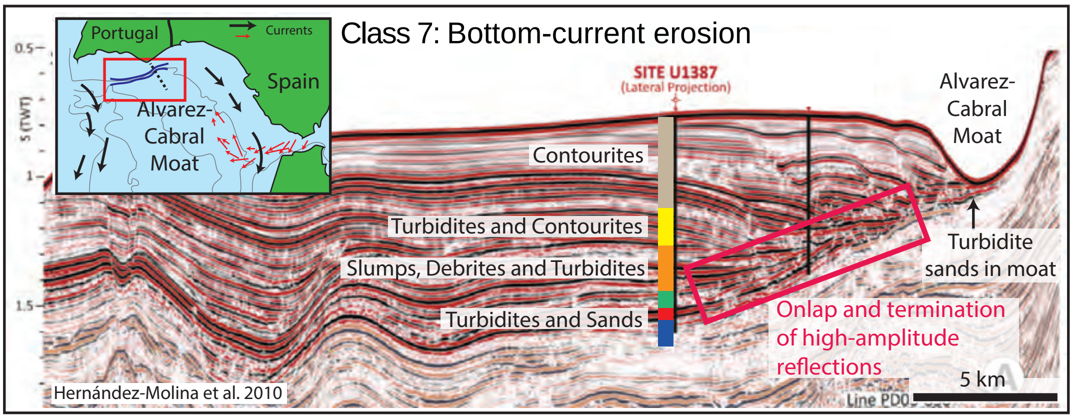

Class 7: Bottom-current erosion
Portugal
Currents
Spain
Alvarez-Cabral Moat
SITE U1387
(Lateral Projection)
Alvarez-Cabral Moat
Contourites
Turbidites and Contourites
Slumps, Debrites and Turbidites
Turbidites and Sands
Turbidite sands in moat
Onlap and termination of high-amplitude reflections
5 km
0.5
1
1.5
s (TWT)
Hernández-Molina et al. 2010

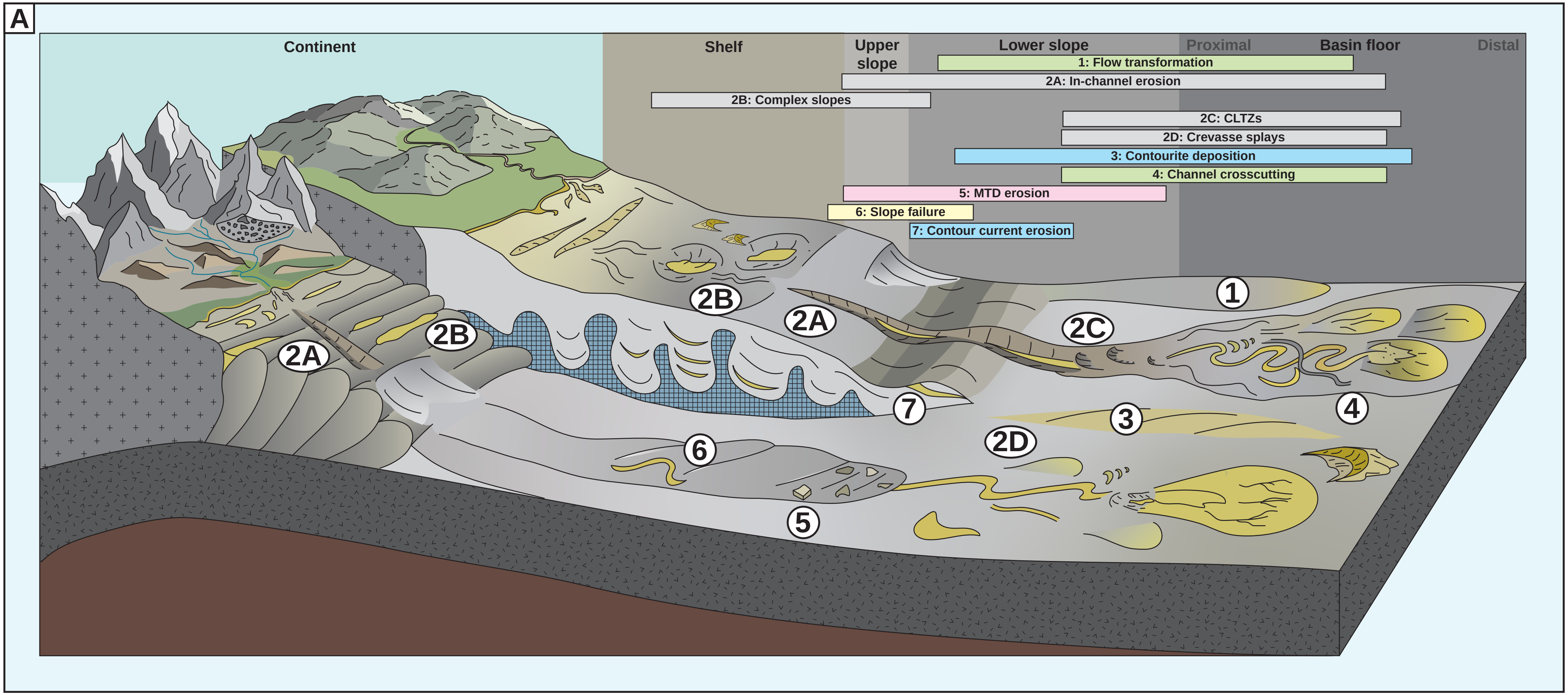


**B**

| Process | Class 1: Flow transformation | Class 2: Turbidity current erosion | Class 3: Contourite deposition | Class 4: Submarine channel erosion | Class 5: MTD erosion | Class 6: Slope failure | Class 7: Contour current erosion |
|---|---|---|---|---|---|---|---|
| **Risks** | Incomplete flow transformation (debrite deposition); unpredictability | High reattachment potential; lag deposition below seismic resolution | Incomplete detachment; small geobody size; low quality sands | Incomplete erosion; Coarse-grained lags in mud-filled channels | Shallow erosion and incomplete detachment | Failure in sandier margins may still result in sand-on-sand contact | Incomplete erosion; scours/moats may be later filled by sands |
| **Subsurface or outcrop example** | Outcrop (Jurassic-Cretaceous) East Greenland Henstra et al., 2016 | Subsurface (Jurassic) North Sea Doré and Robbins, 2005 | Outcrop (Miocene) Morocco Capella et al., 2017 | Subsurface (Cretaceous) Porcupine Basin Providence Resources, 2016 | Subsurface (Neogene/Quaternary) Gulf of Mexico Diaz et al., 2011, Godo 2006 | Subsurface (Cretaceous) Porcupine Basin Pedley et al., 2016 | Erosive processes well-documented in the seafloor subsurface; see Faugeres et al., 1999 |